

On De-Individuated Neurons: Continuous Symmetries Enable Dynamic Topologies

George Bird
Department of Computer Science
& Department of Physics and Astronomy
University of Manchester
george.bird@postgrad.manchester.ac.uk

March 2, 2026

Abstract

This paper introduces a novel methodology for dynamic networks by leveraging an emerging symmetry-principled class of primitives, “isotropic activation functions”. This approach enables real-time neuronal growth and shrinkage of the architectures in response to task demand. This is made possible by network structural changes that are invariant under symmetry reparameterisations, leaving the computation identical under neurogenesis and well approximated under neurodegeneration. This is undertaken by leveraging the isotropic primitives’ property of basis independence, resulting in the loss of the individuated neurons implicit in the elementwise functional form. Isotropy thereby allows a freedom in the basis to which layers are decomposed and interpreted as individual artificial neurons. This enables a layer-wise diagonalisation procedure, in which typical interconnected layers, such as dense layers, convolutional kernels, and others, can be reexpressed so that neurons have one-to-one, ordered connectivity within alternating layers. This indicates which one-to-one neuron-to-neuron communications are strongly impactful on overall functionality and which are not. Inconsequential neurons can thus be removed (neurodegeneration), and new inactive ‘scaffold’ neurons added (neurogenesis) whilst remaining analytically invariant in function. A new tunable model parameter, ‘intrinsic length’, is also introduced to ensure this analytical invariance. This approach mathematically equates connectivity pruning with neurodegeneration. The diagonalisation also offers new possibilities for mechanistic interpretability into isotropic networks, and it is demonstrated that isotropic dense networks can asymptotically reach a sparsity factor of 50% whilst retaining *exact* network functionality. Finally, the construction is generalised, demonstrating a nested functional class for this form of isotropic primitive architectures.

1 Introduction

Neural plasticity in the quantity and connectivity of neurons is biologically advantageous [1, 2, 3] and routinely occurs in the development of the mammalian brain [4, 5, 6, 7]. Shown to improve neural efficiency through controlled pruning [8, 9], whilst enabling the accumulation of knowledge [3, 7], improving robustness [10] and function through growth [11, 7]; it is therefore hypothesised in this work that analogous behaviour within artificial neural networks may be similarly beneficial.

This, too, may include greater efficiency, fewer anomalous computations, and increased capacity — overall, real-time restructuring may enable improved knowledge acquisition and stabilisation. The practical consequences of a network that can adapt its architecture and connectivity in real-time may be transformative.

Contemporary primitives, activation functions, normalisers, optimisers, and more, are constructed using element-wise functional forms. Historically, these functional forms were inspired by biological neural systems [12]: individual neurons communicating to yield collective function. Hence, a basis-dependent decomposition of activation vectors into ‘neuron’-like components, to which elementwise formulae are then applied, reflects this individuated neuron-derived premise. However, due to this individuated neuron construction, architecture adaptation, particularly neurodegeneration, can become difficult if one wishes to closely preserve function due to strong interconnectivity. For contemporary primitives, equivalence classes typically admit only discrete supergroups of permutation symmetries for reparameterisation [13, 14], with few exceptions. This work proposes instead generalising this construction through a symmetry-led approach. These can then be substituted, producing new admissible functional forms and consequential function-invariant reparameterisation. Using this, basis-independent formulations are achieved through orthogonal symmetries, yielding generalised ‘deindividuated’ neurons, since there is no canonical basis for decomposition.

Hence, a novel methodology for dynamic topologies is enabled by leveraging an orthogonal-symmetry-derived alternative formulation of primitives, termed “isotropic primitives” [15], particularly the isotropic activation functions. These alternative non-elementwise primitives enable real-time network restructuring with minimal function degradation, by exploiting basis changes enabled in continuous reparameterisations. Basis-independence ensures that the network remains function-invariant under continuous basis changes. Hence, this work leverages the typical equivalence class under the reparameterisation approach to symmetries, yet this continuous-symmetry reformulation uniquely permits improved neurodegeneration of network architectures beyond what is possible with classical parameter relabelling by using a basis that diagonalises connectivity. Overall, this work indicates both the flexible use cases of these alternative isotropic formulations and enables the exploration of architectural adaptations to new information and learning.

This manuscript presents three key contributions:

1. **Core Conceptual Contribution:** Functional forms, e.g. elementwise, are historically conceptually derived from the notion of individual neurons as fundamental units to compose. From these functional forms, function-invariant symmetries are typically deduced. Instead, this relation can be reversed, with prescribed symmetries determining permitted primitive functional forms. This enables a symmetry-led generalisation to the class of basic functional forms underpinning the *neural* learning systems, and constitutes the broader objective beyond the presented dynamical architectures.
2. **Primitive Reformulations:** Such reversal enables continuous (orthogonal) symmetry defined (isotropic) primitives, a functional form which implicitly generalises the notion of a neuron, by displaying a unique basis-independence absent in elementwise formulae.
3. **Behavioural Implications:** Leveraging such basis-independent primitives allows affine maps to be diagonalised. From this, dynamical architectures are enabled by introducing procedures for neurogenesis and neurodegeneration within the diagonalised representations. This function-invariant diagonalisation also clarifies an asymptotic 50% perfect sparsification possible in networks.

Empirical results of *Sec. 4* demonstrate these dynamic-topology networks on CIFAR10 classification, demonstrating that width can be changed with minimal loss of function. These results also demonstrate the biological phenomena observed in [9], namely that an overabundance of neurons at initialisation, followed by pruning, leads to better-performing networks than those that maintain constant width — a phenomenon that mirrors that of mammalian neural systems.

The subsequent sections expand on the functional form generalisations proposed in more detail, whilst *App. A* situates them in a historical context and explains why generalising to a broader symmetry class may be reasonably undertaken.

2 Theoretical Background on Isotropic Functions and Diagonalisation

This section outlines how a network can be diagonalised to enable growth and pruning under various reparameterisations and conditions. Moreover, considering such an approach allows for a network to be sparsified asymptotically to 50% of its original number of weights, without *any* loss in functionality.

First, a general introduction to isotropic activation functions is given. These considerations also apply if isotropic normalisations are used. Following this, a layer-wise basis change to a diagonalised configuration using singular-value decomposition will be described, along with a more efficient partial diagonalisation procedure for training-time. Concluded in the subsequent theory section is an implementation of how a network can undergo growth and pruning for each layer, and a brief discussion of applications.

2.1 Introduction to Isotropic Activation Functions (Orthogonal-Group Defined)

Isotropy is most generally an orthogonal group family constraint applied to form a set of primitives. This generalised constraint can form activation functions, normalisers, initialisers, and optimisers with the same underlying symmetry properties [15] and argued network-wide implications, particularly on representations [16, 17].

These primitives transform under a particular, typically standard, representation of the orthogonal group specific to the width of the layer. In this section, activation functions and normalisers are the primary concern¹.

For the primitives in this scenario, and for an n -width network, the standard representation is given by $\rho : \mathcal{O}(n) \rightarrow \text{GL}_n(\mathbb{R})$ and each element will be notated as a matrix $\mathbf{R} = \rho(g) \in \text{GL}_n(\mathbb{R})$ where g is an element of the orthogonal group, $g \in \mathcal{O}(n)$. This is just the standard $\mathbb{R}^{n \times n}$ representation for orthogonal (rotation-like) matrices. The representation theoretic notation will be suppressed moving forward for approachability to $\mathbf{R} \in \mathcal{O}(n)$.

For the isotropic activation functions functional class of study, $\mathbf{f} \in \mathcal{F}$, they are defined by actions of this group commuting with the isotropic functional form, $\mathbf{f} : \mathbb{R}^n \rightarrow \mathbb{R}^n$, as shown in *Eqn. 1*. Additionally, it is essential that these functions *maximally* abide by this group’s symmetry.

¹Within this framework, the definitional distinctions between activation functions and normalisers become less clear; for example, Layer-Normalisation could be considered a parameterised activation function with a specific symmetry constraint [18]. Therefore, a proposed distinguishing difference defining normalisers is proposed to be the presence of probabilistic constraints, time-like or data-like, and whether representative degrees-of-freedom are lost as a normaliser or preserved as an activation function.

$$\forall \mathbf{R} \in O(n) \quad [\mathbf{R}, \mathbf{f}] = \mathbf{R} \circ \mathbf{f} - \mathbf{f} \circ \mathbf{R} = 0 \quad (1)$$

More straightforwardly, it can be denoted as shown in Eqn. 2.

$$\mathbf{f}(\mathbf{R}\vec{x}) = \mathbf{R}\mathbf{f}(\vec{x}) \quad (2)$$

From this constraint, the activation function class can be constructed for this symmetry-defined primitive. A functional form which is within this functional class is displayed in Eqn. 3, where \hat{x} is the unit-normalised vector given the 2-norm².

$$\mathbf{f}(\vec{x}) = f(\|\vec{x}\|_2) \hat{x} \quad (3)$$

Many functions, which are non-linear in f , maximally satisfy this relation. The particularities of *which function is used do not matter for dynamic network topologies*.

Several placeholders are suggested [15]; however, these superficially replicate existing activation functions, and there is no reason to assume their continued optimality in this altered function form. Therefore, the general function will just be denoted as $\mathbf{f}(\vec{x}) = \sigma(\|\vec{x}\|) \hat{x}$. This equivariance is demonstrated in Eqns. 4 to 7, using $\vec{x}' = \mathbf{R}\vec{x}$ for orthogonal matrix \mathbf{R} and that $\hat{x}' = \mathbf{R}\hat{x}$ remains unit-normalised.

$$\mathbf{f}(\vec{x}') = \sigma(\|\vec{x}'\|) \hat{x}' = \sigma(\|\mathbf{R}\vec{x}\|) \mathbf{R}\hat{x} = \mathbf{f}(\mathbf{R}\vec{x}) \quad (4)$$

$$\sigma(\|\mathbf{R}\vec{x}\|) \mathbf{R}\hat{x} = \sigma\left(\sqrt{\vec{x}^T \mathbf{R}^T \mathbf{R} \vec{x}}\right) \mathbf{R}\hat{x} \quad (5)$$

$$\mathbf{R}\sigma\left(\sqrt{\vec{x}^T \mathbf{I}_n \vec{x}}\right) \hat{x} = \mathbf{R}\sigma(\|\vec{x}\|) \hat{x} \quad (6)$$

$$\therefore \mathbf{f}(\mathbf{R}\vec{x}) = \mathbf{R}\mathbf{f}(\vec{x}) \quad (7)$$

2.2 Single-Sided Continuous Reparameterisations

This paper employs diagonalisation of layers for its dynamic topology method. This can most clearly be seen when two such orthogonal functions, or more sequential orthogonal primitives, are composed with *three* affine layers. This is a distinct compositional consideration from parameter symmetry work, which typically focuses on a single discrete permutation activation function sandwiched by two affine layers and is discussed briefly in this subsection. In effect, the full diagonalisation considers the *continuous* orthogonal reparameterisations twice, concurrently acting on the left and right of the middle affine layer.

This reparameterisation is possible due to the functional class of affine layers exhibiting left and right closure under general linear actions — ‘closure’ as defined through the previously proposed symmetry taxonomy [15]. Since the orthogonal group is a subset of the general linear group, the affine layer is closed under orthogonal actions. It can therefore be reparameterised to produce an equivalence class of functionally identical models. Combining this with orthogonal equivariance enables a reparameterisation where the network’s functionality remains exactly invariant — all aspects of the network’s output function with respect to any input are preserved.

This derivation is demonstrated in the transformations between Eqns. 8 through 12, where $\mathbf{f}_{\text{Aff.1}}(\vec{x}) = \mathbf{W}_1 \vec{x} + \vec{b}_1$ and $\mathbf{f}_{\text{Aff.2}}(\vec{x}) = \mathbf{W}_2 \vec{x} + \vec{b}_2$ and $\mathbf{f}_{\text{Iso.}} = \sigma(\|\vec{x}\|) \hat{x}$, and using the relation $\mathbf{I}_n = \mathbf{R}^{-1} \mathbf{R} = \mathbf{R}^T \mathbf{R}$ for orthogonal matrices. This is for the standard two-affine with one non-linearity reparameterisation.

$$\mathbf{f}_{\text{Aff.2}} \circ \mathbf{f}_{\text{Iso.}} \circ \mathbf{f}_{\text{Aff.1}} = \mathbf{W}_2 \mathbf{f}\left(\mathbf{W}_1 \vec{x} + \vec{b}_1\right) + \vec{b}_2 \quad (8)$$

$$= \mathbf{W}_2 \mathbf{f}\left(\mathbf{R}^T \mathbf{R}\left(\mathbf{W}_1 \vec{x} + \vec{b}_1\right)\right) + \vec{b}_2 \quad (9)$$

$$= \underbrace{\mathbf{W}_2 \mathbf{R}^T}_{\mathbf{W}'_2} \mathbf{f}\left(\underbrace{\mathbf{R} \mathbf{W}_1}_{\mathbf{W}'_1} \vec{x} + \underbrace{\mathbf{R} \vec{b}_1}_{\vec{b}'_1}\right) + \vec{b}_2 \quad (10)$$

$$= \mathbf{W}'_2 \mathbf{f}\left(\mathbf{W}'_1 \vec{x} + \vec{b}'_1\right) + \vec{b}_2 \quad (11)$$

²One may notice the 2-norm present in this description and wonder whether this approach can be generalised to l -norm. Although appropriate primitive redefinition can be achieved using this to provide functional classes within the hyperoctahedral B_n primitive set, these considerations do not generalise well to dynamic network topologies. One may consider adapting the singular value decomposition (SVD) diagonalisation procedure such that orthogonal group matrices are defined with a unit-norm defined by $\|\vec{a}\|_n$; however, there is a lack of an inner-product inducing the norm. This means that the l -norm does not define a generalised orthogonality, so one has to use the standard inner product. This leaves only the discrete hyperoctahedral group to which the map is equivariant, and it lacks the continuous group needed for this approach to project down to smaller subspaces. Although if all incoming weights to a neuron tend to zero, then it can still be pruned. Growth remains possible regardless.

$$= \mathbf{W}'_2 \mathbf{f} \left(\mathbf{W}'_1 \vec{x} + \vec{b}'_1 \right) + \vec{b}'_2 = \mathbf{f}'_{\text{Aff.2}} \circ \mathbf{f}_{\text{Iso.}} \circ \mathbf{f}'_{\text{Aff.1}} \quad (12)$$

When considering the full three affine and two non-linearity compositional scenarios, a layer can be fully diagonalised by applying such transformations to the left and right of the intermediate affine layer, isolating a sparse and simply-connected diagonalised matrix within the central affine layer. This diagonalisation is achieved through a singular value decomposition allowed through this two-sided gauge freedom. The diagonalised weights can then be ordered by singular value magnitude, enabling a perturbative consideration of the layer's action — especially when incorporating normalisation. This diagonalisation procedure is discussed in the following subsection.

2.3 Layer Diagonalisation

First, a procedure for fully diagonalising a layer will be demonstrated. This makes clear that one layer at a time can be reparameterised to express a one-to-one connectivity between the current layer's neurons, individuated in a particular basis, and the preceding layer's neurons. For a full diagonalisation, as stated, this requires three affine layers interspaced around two isotropic primitives. However, growth and pruning of the network do not necessarily require a full diagonalisation. For efficiency, several matrices can be contracted in an abridged approach to the method. The latter partial diagonalisation using singular value decomposition will be discussed following the full diagonalisation.

Similar to before, one can consider two isotropic activation functions, or generally non-linearity, interspaced with three affine maps:

- First Affine Layer: $\mathbf{f}_{\text{Aff.1}} : \mathbb{R}^l \rightarrow \mathbb{R}^m$. A functional class with form $\mathbf{f}_{\text{Aff.1}}(\vec{x}) = \mathbf{W}_1 \vec{x} + \vec{b}_1$. Has both left and right general-linear closure (functional class) symmetries; the left closure will be utilised.
- First Non-Linearity: $\mathbf{f}_{\text{Iso.1}} : \mathbb{R}^m \rightarrow \mathbb{R}^m$. A functional class with form $\mathbf{f}_{\text{Iso.1}}(\vec{x}) = \sigma_1(\|\vec{x}\|) \hat{x}$. Exhibits a standard orthogonal algebraic equivariance symmetry by definition; this will be leveraged.
- Second Affine Layer: $\mathbf{f}_{\text{Aff.2}} : \mathbb{R}^m \rightarrow \mathbb{R}^n$. A functional class with form $\mathbf{f}_{\text{Aff.2}}(\vec{x}) = \mathbf{W}_2 \vec{x} + \vec{b}_2$. Has both left and right general-linear closure (functional class) symmetries; both closures will be utilised.
- Second Non-Linearity: $\mathbf{f}_{\text{Iso.2}} : \mathbb{R}^n \rightarrow \mathbb{R}^n$. A functional class with form $\mathbf{f}_{\text{Iso.2}}(\vec{x}) = \sigma_2(\|\vec{x}\|) \hat{x}$. Exhibits a standard orthogonal algebraic equivariance symmetry by definition; this will be leveraged.
- Third Affine Layer: $\mathbf{f}_{\text{Aff.3}} : \mathbb{R}^n \rightarrow \mathbb{R}^o$. A functional class with form $\mathbf{f}_{\text{Aff.3}}(\vec{x}) = \mathbf{W}_3 \vec{x} + \vec{b}_3$. Has both left and right general-linear closure (functional class) symmetries; the right closure will be utilised.

With their composition specified by: $\mathbf{f}_{\text{Aff.3}} \circ \mathbf{f}_{\text{Iso.2}} \circ \mathbf{f}_{\text{Aff.2}} \circ \mathbf{f}_{\text{Iso.1}} \circ \mathbf{f}_{\text{Aff.1}} : \mathbb{R}^l \rightarrow \mathbb{R}^o$. Then $\mathbf{f}_{\text{Aff.2}}$ can be reexpressed in a basis where it becomes diagonalised and ordered by singular values. The diagonalisation transformations are displayed in *Eqns. 13 to 17*, which act on the intermediate affine layer with a double-sided transformation similar to the previous section's reparameterisation. In particular, the weights \mathbf{W}_2 can be represented with a singular value decomposition $\mathbf{W}_2 = \mathbf{U} \Sigma_2 \mathbf{V}^T$, where \mathbf{U} and \mathbf{V} are orthogonal so can commute with the non-linearity orthogonal equivariance symmetry by construction, and Σ_2 is a diagonal matrix.

$$\mathbf{W}_3 \mathbf{f}_{\text{Iso.2}} \left(\mathbf{W}_2 \mathbf{f}_{\text{Iso.1}} \left(\mathbf{W}_1 \vec{x} + \vec{b}_1 \right) + \vec{b}_2 \right) + \vec{b}_3 \quad (13)$$

$$= \mathbf{W}_3 \mathbf{f}_{\text{Iso.2}} \left(\mathbf{U} \Sigma_2 \mathbf{V}^T \mathbf{f}_{\text{Iso.1}} \left(\mathbf{W}_1 \vec{x} + \vec{b}_1 \right) + \underbrace{\mathbf{U} \mathbf{U}^T}_{\mathbf{I}_n} \vec{b}_2 \right) + \vec{b}_3 \quad (14)$$

$$= \mathbf{W}_3 \mathbf{U} \mathbf{f}_{\text{Iso.2}} \left(\Sigma_2 \mathbf{f}_{\text{Iso.1}} \left(\mathbf{V}^T \left(\mathbf{W}_1 \vec{x} + \vec{b}_1 \right) \right) + \mathbf{U}^T \vec{b}_2 \right) + \vec{b}_3 \quad (15)$$

$$= \underbrace{\mathbf{W}_3 \mathbf{U}}_{\mathbf{W}'_3} \mathbf{f}_{\text{Iso.2}} \left(\Sigma_2 \mathbf{f}_{\text{Iso.1}} \left(\underbrace{\mathbf{V}^T \mathbf{W}_1}_{\mathbf{W}'_1} \vec{x} + \underbrace{\mathbf{V}^T \vec{b}_1}_{\mathbf{b}'_1} \right) + \underbrace{\mathbf{U}^T \vec{b}_2}_{\vec{b}'_2} \right) + \vec{b}_3 \quad (16)$$

$$= \mathbf{W}'_3 \mathbf{f}_{\text{Iso.2}} \left(\Sigma_2 \mathbf{f}_{\text{Iso.1}} \left(\mathbf{W}'_1 \vec{x} + \mathbf{b}'_1 \right) + \vec{b}'_2 \right) + \vec{b}_3 \quad (17)$$

This reparameterisation corresponds to the following transforms for the modified affine layers.

$$\begin{aligned} \mathbf{W}'_1 &= \mathbf{V}^T \mathbf{W}_1 & \mathbf{W}'_2 &= \mathbf{U}^T \mathbf{W}_2 \mathbf{V} = \mathbf{U}^T \mathbf{U} \Sigma_2 \mathbf{V}^T \mathbf{V} = \Sigma_2 & \mathbf{W}'_3 &= \mathbf{W}_3 \mathbf{U} \\ \vec{b}'_1 &= \mathbf{V}^T \vec{b}_1 & \vec{b}'_2 &= \mathbf{U}^T \vec{b}_2 & \vec{b}'_3 &= \vec{b}_3 \end{aligned} \quad (18)$$

Where \mathbf{W}'_2 is now fully diagonalised, in effect the 'neurons' from this perspective only communicate one-to-one in this layer, as depicted in *Fig. 1*. This greatly simplifies the construction and may aid in isotropic network interpretability.

This is because the generalised neuron is non-individuated, expressing a gauge freedom for reparameterisation in many differing and equivalent bases, hence resulting in an analytically identical computation. In other words, the choice of individual neurons is arbitrary, as there is no map which individuates them so can be chosen in a convenient expression.

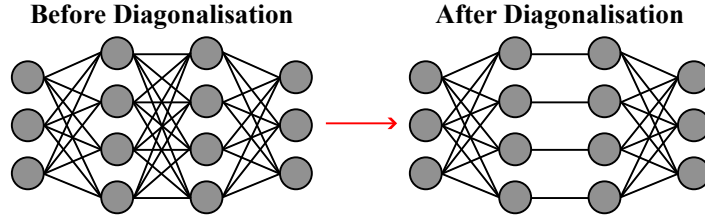


Figure 1: This illustration depicts the qualitative effects on a network from full diagonalisation — the chosen layer has a double-sided basis change to the connectivity, reducing the map to a one-to-one correspondence between neurons. This drastically simplifies the interrelations between the chosen layer, allowing the application of the dynamic network implementation. In general, for sequential layers, only one layer can be diagonalised at a time, as diagonalising one layer often destroys the diagonalised state of the immediately preceding and following layers in the process. Layers which are interspaced by other affine transforms can be concurrently diagonalised.

Additionally, this decomposition can be computed whilst ordering the singular values. This can give an indication of the importance of each weight and will be leveraged throughout the following methodology. Regularisation could be applied to these singular values as a form of weight decay if desirable. One may be concerned that the one-to-one connectivity of layers infers a suboptimality of these layers; however, this is not necessarily so, as one can still analyse classical anisotropic networks with their parameters reexpressed as a diagonalised spectrum of one-to-one connections, it is just not possible to reparameterise the model in such a way as it does not commute with the elementwise operations. Therefore, this does not necessarily imply a lack of expressibility.

2.3.1 Comment on Sparsity of Diagonalisation

Incidentally to this full layer diagonalisation intended for dynamical networks, one can observe that this reparameterisation can also be leveraged to convert the existing network into a sparser basis, whilst preserving the function exactly.

The approach above enables every other layer of a multilayer perceptron, and potentially generalised across other architectures, to be reexpressed in a diagonalised parameterisation whilst retaining all performance. This may be important for both efficiency and mechanistic interpretability.

If one considers a dense network with all layers of n -width, this would ordinarily consist of $N(N + 1)$ parameters per affine mapping — N^2 for weights and N for biases³. However, if that layer is able to be diagonalised, then the affine transform can be equally described by just $2N$ parameters. Incidentally, to the objective of this paper, this can be considered a vast improvement in sparsity of the dense network without *any* performance loss. The map is now equivalent to an elementwise product and summation. This grows linearly with neuron size as opposed to quadratically (typically bilinearly).

Naturally, this must be associated with two additional affine layers to enable such a reparameterisations. Nevertheless, this sparsity is a drastic computational improvement, particularly for a static inference-time network, unlike the naive parameterisation. Moreover, the full diagonalisation can be computed for every alternative layer surrounded by non-diagonalised affine layers. For an (odd-length) dense network, with n -width layers and $2D + 1$ sequential affine mappings, then Eqn. 19 gives the sparsity factor S_p . This is the proportion of remaining parameters compared to the original count. Even-length networks have a similar relation with slightly higher sparsity.

$$S_p = \frac{2DN + N(D + 1)(N + 1)}{N(2D + 1)(N + 1)} = \frac{D + 1}{2D + 1} + \frac{2D}{(2D + 1)(N + 1)} \quad (19)$$

Thus, the network can be reexpressed in a sparsified basis, with a proportion of parameters that is equal to a constant plus a term which drops reciprocally with layer width, as one may expect. Asymptotically, as $D \rightarrow \infty$ and $N \rightarrow \infty$, **the network preserves an exact function with only 50% of the parameters.**

Moreover, this may be further improved by jointly optimising over all of the layerwise basis changes, such as to maximise the overall sparsity across all parameters instead of every alternative layer. Therefore, Eqn. 19 provides an indication of sparsity for odd-length dense isotropic networks. Further sparsification may be achieved through working with the direct sum of parameterised orthogonal groups, such as through their Lie algebras and optimising for elementwise sparsity to leverage sparse-matrix computations.

Both of these approaches yield exact analytical sparsification, which is a symmetry-leveraged structural, not statistical, sparsity mask. However, from these parameterisations, the already symmetry-sparsified network can serve as a base from which to then perform classical sparsifying of the parameters. Hence, allowing some approximation of function, this

³Additional parameters for isotropic normalisations or other operations may be present.

sparsity factor may be drastically improved using conventional methodologies of pruning — moreover, the singular values in already diagonalised layers can aid in an analysis of the function approximation (particularly when using a form of normalisation to ensure magnitude compensation does not occur in the subsequent layer). This is felt to be a worthwhile and exciting direction for isotropic networks, which already show some preliminary improved performance on some tasks [17].

2.3.2 Partial Layer Diagonalisation

Despite being illustrative and perhaps more broadly practical and interpretable, the full diagonalisation procedure is not necessary for dynamic topologies. The proposed algorithm for dynamic topologies can proceed with a simplified form, which may be more practical. This reparameterisation follows more closely the standard two affine layers surrounding an (isotropic) non-linearity. This partial diagonalisation can occur in two forms: left-sided and right-sided, corresponding to the following parameterised maps: mixing followed by scaling or scaling followed by mixing, respectively. The right-sided transform is explicitly given in *Eqns.* 20 through 24. This also influences which direction the pruning and growth acts, forward or backwards, which are both permissible applications under this construction. However, the forward approach exhibits the most versatility.

$$\mathbf{W}_2 \mathbf{f}_{\text{iso},1} \left(\mathbf{W}_1 \vec{x} + \vec{b}_1 \right) + \vec{b}_2 \quad (20)$$

$$= \mathbf{W}_2 \mathbf{f}_{\text{iso},1} \left(\mathbf{U} \Sigma_1 \mathbf{V}^T \vec{x} + \underbrace{\mathbf{U} \mathbf{U}^T}_{\mathbf{I}_n} \vec{b}_1 \right) + \vec{b}_2 \quad (21)$$

$$= \mathbf{W}_2 \mathbf{U} \mathbf{f}_{\text{iso},1} \left(\Sigma_1 \mathbf{V}^T \vec{x} + \mathbf{U}^T \vec{b}_1 \right) + \vec{b}_2 \quad (22)$$

$$= \underbrace{\mathbf{W}_2 \mathbf{U}}_{\mathbf{W}'_2} \mathbf{f}_{\text{iso},1} \left(\underbrace{\Sigma_1 \mathbf{V}^T}_{\mathbf{W}'_1} \vec{x} + \underbrace{\mathbf{U}^T}_{\vec{b}'_1} \vec{b}_1 \right) + \vec{b}_2 \quad (23)$$

$$= \mathbf{W}'_2 \mathbf{f}_{\text{iso},1} \left(\mathbf{W}'_1 \vec{x} + \vec{b}'_1 \right) + \vec{b}'_2 \quad (24)$$

This right partial diagonalisation is given by the following reparameterisations, which correspond to a modified affine layers:

$$\begin{aligned} \mathbf{W}'_1 &= \mathbf{U}^T \mathbf{W}_1 = \mathbf{U}^T \mathbf{U} \Sigma_1 \mathbf{V}^T = \Sigma_1 \mathbf{V}^T & \vec{b}'_1 &= \mathbf{U}^T \vec{b}_1 \\ \mathbf{W}'_2 &= \mathbf{W}_2 \mathbf{U} & \vec{b}'_2 &= \vec{b}_2 \end{aligned} \quad (25)$$

This partial diagonalisation is sufficient to prune and grow neurons defined by the layer to which $\mathbf{f}_{\text{iso},1}$ applies over. It does require that the diagonalised matrix Σ_1 be retained for the thresholding. Overall, this partial diagonalisation is sufficient for the methodology, but not as illustrative as the full diagonalisations, where the one-to-one mapping is explicit, sparsified and better interpretable. Both methods remain applicable for the procedures presented, with the latter partial diagonalisation enabling dynamic topologies additionally in the first layer, since no preceding layer needs to ‘absorb’ the \mathbf{V} orthogonal matrix. Hence, full-diagonalisation is not possible on this first layer; however, prior work suggests that pruning of the first layer is disproportionately unfavourable to performance anyway [19] — this would require reestablishing such an empirical finding again for isotropic networks due to their foundational and representational distinctions. Additionally, partial diagonalisation may offer short-term improvement in efficiency due to fewer matrix multiplications, though full-diagonalised sparsified reparameterisation may remain preferable at inference time. For clarity, the full diagonalisation will be referenced moving forward; however, code implementations use the partial form to additionally enable growth and pruning of the first hidden layer.

3 Theory of Isotropic Dynamical Networks

3.1 Dynamic Pruning

Considering the intermediate affine map $\mathbf{f}_{\text{Aff},2}$, which has been expressed in a diagonalised basis with weights ordered as singular values, $\mathbf{W}'_2 = \Sigma \in \mathbb{R}^{n \times m}$, $\Sigma_{ii} \geq \Sigma_{(i+1)(i+1)}$. As this diagonalised weight tends to zero, the ‘neuron’ becomes entirely independent of the preceding layer, $\Sigma_{ii} \rightarrow 0$. This enables the pruning of the entire neuron, not just a single connection, since the neuron has only a single one-to-one connectivity due to diagonalisation so the connectivity and neuron become one of the same. This pruning results in minimal and measurable degradation of network functionality⁴.

⁴It is suggested to use some form of isotropic normaliser to ensure magnitude-compensations do not occur in subsequent layers. Moreover, this should not be one which suppresses radial degrees-of-freedom in representation, as discussed in *App. C*, instead the previously proposed Chi-normaliser [15] may be well-suited.

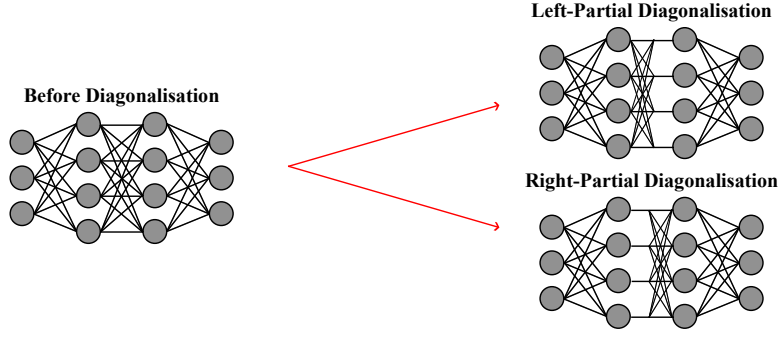


Figure 2: This illustration depicts the qualitative effects on a network from partial diagonalisation. This time, the chosen layer has a single-sided basis change to the connectivity. Depending on the transform side, left- or right-sided, an initial or later mixing of connectivities occurs, followed by scaling by the singular values. This setup may be more convenient to implement than a full diagonalisation. Some interpretability and explanatory convenience are lost due to the remaining connectivity mixing.

Additionally, this is a singular-value-based thresholding for neural pruning as opposed to top- k or thresholded-magnitude based connectivity pruning as commonly implemented⁵.

However, in the current construction, a bias parameter remains and cannot be simply ‘gauged away’ under this reparameterisation. This requires the addition of a new tunable parameter, the “intrinsic length parameter”, denoted o , and there are numerous ways to interpret such a parameter, and its behaviour is largely unique to isotropic networks. This additional parameter has become a crucial additional insight into isotropic networks which enables this unique structural reparameterisation.

To gauge away residual bias into the intrinsic length requires reexpressing the isotropic function, as detailed in Eqns. 26.

$$\mathbf{f}(\vec{x}) = f(\|\vec{x}\|) \hat{x} = f(\|\vec{x}\|) \frac{\vec{x}}{\|\vec{x}\|} = \frac{f(\|\vec{x}\|)}{\|\vec{x}\|} \vec{x} = g(\|\vec{x}\|) \vec{x} \quad (26)$$

Additionally expressing the affine layer as $\Sigma\vec{x} + \vec{b}$ and implementing into Eqn. 26 to yield Eqn. 27.

$$\mathbf{f}(\vec{x}) = g\left(\left\|\Sigma\vec{x} + \vec{b}\right\|\right) \left(\Sigma\vec{x} + \vec{b}\right) \quad (27)$$

One can then expand the norm-term as shown in Eqn. 28 where $\Sigma_{ii} \rightarrow 0$ and \vec{b}_i indicate the i^{th} components decomposed in the standard basis.

$$\left\|\Sigma\vec{x} + \vec{b}\right\|_2^2 = \sum_{j=0}^{\min(n,m)} \left(\Sigma_{jj}\vec{x}_j + \vec{b}_j\right)^2 = \left(\Sigma_{ii}\vec{x}_i + \vec{b}_i\right)^2 + \sum_{i \neq j=0}^{\min(n,m)} \left(\Sigma_{jj}\vec{x}_j + \vec{b}_j\right)^2 = \vec{b}_i^2 + \sum_{i \neq j=0}^{\min(n,m)} \left(\Sigma_{jj}\vec{x}_j + \vec{b}_j\right)^2 \quad (28)$$

As $\Sigma_{ii} \rightarrow 0$, the network’s norm term becomes asymptotically functionally identical to a network of a smaller ‘pruned’ size, except for the residual bias \vec{b}_i . The residual \vec{b}_i in the linear part of the isotropic activation function can be forward projected to update the biases of the following affine layer, such that it identically cancels; however, the \vec{b}_i within the norm cannot.

This requires a new tunable parameter: ‘intrinsic length’, which can ‘absorb’ the bias, making the network asymptotically exhibit full invariance to the action of pruning. This intrinsic length is assumed to be positive definite $o = \exp(\lambda)$ such that isotropic activation functions such as isotropic-tanh [15] remain defined as intended; however, this positive-definite property is not a strict requirement if the isotropic non-linearity is designed to permit it. Therefore, this intrinsic length can be generalised but will be assumed to be positive in the following discussion. Crucially, it can also be made trainable as a novel optimisable parameter specific to isotropic networks.

Geometrically, it acts much like a bias that is orthogonal to the linear space. An intuition is that it is embedding the existing subspace away from the origin, e.g. $(\Sigma\vec{x} + \vec{b})^T \vec{o}_\perp = 0$ and $\vec{o}_\perp^T \vec{o}_\perp = o = \exp(\lambda)$ — where λ can be instead optimised to ensure positive definiteness. If interpreted in such a geometric picture, the associated offset vector does exhibit a rotational degeneracy in the orthogonal complement space. Except for the following activation function, this complement space is projected out before the following affine layer. This returns the vector space to its prior dimensionality.

⁵However, it is stressed that any of the previous approaches to decide connection-pruning may be similarly applicable, and can be explored empirically. This singular-value thresholding is presented merely as a novel alternative and may not be optimal; however, it will be assumed moving forward. In practice, the methodology is to be kept open to any alternative thresholding schemes, such as additionally using gradients, which may be preferable in many circumstances. Similarly, one may combine approaches and consider the gradient with respect to the diagonalised singular value as a threshold for pruning — this is also effectively a batch statistic. However, naturally, pruning should always begin with the smallest singular value or loss-gradient magnitude to avoid function degradation.

Overall, the intrinsic length offers a novel and beneficial trainable parameter for an isotropic network analogous to a perpendicular bias. If allowed to be negative, it may allow direction flipping, which may increase network support for manipulating representations into antipodal arrangements where desirable. It could also be reinterpreted as a parameterised activation function instead of an additional orthogonal offset parameter for the affine map.

In Eqn. 29, the norm is generalised with this new parameter.

$$\left\| \Sigma \vec{x} + \vec{b} + \vec{\sigma}_\perp \right\|_2^2 = \underbrace{\vec{\sigma}_\perp^T \vec{\sigma}_\perp}_{=o' = \vec{\sigma}_\perp^T \vec{\sigma}_\perp} + \sum_{j=0}^{\min(n,m)} \left(\Sigma_{jj} \vec{x}_j + \vec{b}_j \right)^2 = \underbrace{o + \vec{b}_i^2}_{=o' = \vec{\sigma}_\perp^T \vec{\sigma}_\perp} + \sum_{\substack{j=0 \\ j \neq i}}^{\min(n,m)} \left(\Sigma_{jj} \vec{x}_j + \vec{b}_j \right)^2 = \left\| \Sigma' \vec{x} + \vec{b}' + \vec{\sigma}'_\perp \right\|_2^2 \quad (29)$$

It can also be shown that this remains invariant to orthogonal group actions, preserving the overall isotropic activation function’s equivariance, $\mathbf{f}_{\text{iso.}}(\mathbf{R}\vec{x}) = \mathbf{R}\mathbf{f}_{\text{iso.}}(\vec{x})$.

Overall, this additional parameter enables one to ‘gauge away’ residual bias using parameter degrees-of-freedom, further minimising function degradation during whole neuron pruning. This accounts for the normalisation term, but the linear aspect can be similarly accounted for through reparameterisation of the subsequent layer accommodating the pruned bias into the subsequent biases.

However, functional degradation does remain when the pruned diagonalised weight is not identically zero, but close to: $\Sigma_{ii} = \epsilon$ with $0 < \epsilon \ll 1$. As stated, this should be mitigated using an isotropic normalisation composed with the activation function. Typically, one may attempt the standard approaches, layer-normalisation and batch-normalisation; however, isotropic alternatives are instead required. The latter is particularly discussed in App. C, which had the additional consequence of revealing an isotropic architecture which inherently displays a depthwise nested functional class due to the isotropic terms. This is felt to be rather significant as it reproduces the nested functional class structure in an alternative way to the typical Residual Network construction, and in a way which doesn’t constrain layer dimensionality. Instead, it is a natural consequence of the symmetry-principled reformulations of primitives.

In summary, generalising layer-normalisation to isotropy requires one not to normalise by the mean, as this results in a change in intrinsic geometry: $\mathbb{R}^n \rightarrow \mathbb{R}^{n-1} \hookrightarrow \mathbb{R}^n$ [15], while dividing by the standard deviation projects to a hyper-spherical shell. In App. C this is shown to result in affine expressibility of the network, rendering it limited in its application. Therefore, a batch-normaliser such as the Chi-normaliser [15] may be employed to reduce function degradation under pruning.

Additionally, this forward correction for the bias in the linear term (\vec{x} of $g(\|\vec{x}\|)\vec{x}$) is similarly applicable to any remaining $\Sigma_{ii} = \epsilon$ term producing \vec{x} . If one considers the linear term, with original diagonalised weights Σ and its pruned form Σ' alongside subsequent weight matrix before and after pruning, $\mathbf{W}^{(2)}$ and $\mathbf{Y}^{(2)}$ respectively, then we desire the following map to be closely preserved: $\mathbf{Y}^{(2)}\Sigma'\vec{x} \approx \mathbf{W}^{(2)}\Sigma\vec{x}$. Therefore, one can find a suitable adjusted weight $\mathbf{Y}^{(2)}$ through a moore-penrose pseudo-inverse, where rank permits, such as to minimise a least-squares difference in these maps. This is displayed in Eqn. 30, when an inverse can be determined (if not, one may continue to use the original $\mathbf{W}^{(2)}$ with the associated column pruned.). If it is the smallest singular value which is deleted, as intended, then this reduces to a corresponding column deletion of $\mathbf{Y}^{(2)}$ as would expected — since removing the smallest singular value and associated parameters minimally changes the mapping. Hence, this can be considered to derive the subsequent layer’s columnwise deletion. This will be further detailed in Sec. 3.3 which outlines the overall implementation.

$$\mathbf{Y}^{(2)} = \mathbf{W}^{(2)}\Sigma\Sigma'^T \left(\Sigma'\Sigma'^T \right)^{-1} \quad (30)$$

3.2 Dynamic Growth

Dynamic growth is comparatively trivial. If acting forwards, it amounts to embedding the last layer’s space into a higher dimensional vector space.

This may be interpreted in two ways for its implications on neurons. The first is that if neurons are chosen to be individuated in some arbitrary basis, it corresponds to appending additional neurons to this layer which are connected in such a manner that the model is functionally independent of them — these could be considered ‘scaffold neurons’ in this conventional individuated picture. Alternatively, it is comparable to treating the higher-dimensional generalised notion of a neuron to have further increased in dimensionality.

Due to the isotropic activation function’s Jacobian acting to distribute learning gradients, *alongside standard connectivity mixing*, these apparent individuated neurons may be rapidly trained despite being functionally independent of the original model. This is because they are a symmetrical reparameterisation with respect to the forward pass, but non-trivially breaks the structural symmetry of the backward pass. This can occur even when connecting parameters are zeroed. This can be seen comparatively for a typical anisotropic activation function’s diagonal Jacobian compared to an isotropic non-diagonal Jacobian in Eqns. 31 and Eqn. 32 respectively for a n -‘neuron’ layer, $\mathbf{f} : \mathbb{R}^n \rightarrow \mathbb{R}^n$ and standard basis-vectors \hat{e}_i . The singularity at $\vec{x} = \vec{0}$ can become a non-troublesome coordinate singularity under suitable choices of σ , $\mathbf{f}(\vec{0}) = \vec{0}$

$$\mathbf{f}(\vec{x}) = \sum_{i=1}^N \sigma(\vec{x} \cdot \hat{e}_i) \hat{e}_i \Rightarrow \frac{\partial(\mathbf{f} \cdot \hat{e}_i)}{\partial(\vec{x} \cdot \hat{e}_j)} = \sigma'(\vec{x} \cdot \hat{e}_i) \delta_{ij} \quad (31)$$

$$\mathbf{f}(\vec{x}) = \sigma(\|\vec{x}\|) \hat{x} \Rightarrow \frac{\partial(\mathbf{f} \cdot \hat{e}_i)}{\partial(\vec{x} \cdot \hat{e}_j)} = \frac{\sigma(\|\vec{x}\|)}{\|\vec{x}\|} \delta_{ij} + \left(\sigma'(\|\vec{x}\|) - \frac{\sigma(\|\vec{x}\|)}{\|\vec{x}\|} \right) \frac{(\vec{x} \cdot \hat{e}_i)(\vec{x} \cdot \hat{e}_j)}{\|\vec{x}\|^2} \quad (32)$$

Below, Eqn. 33, shows a reformulated isotropic activation function and its Jacobian.

$$\mathbf{f}(\vec{x}) = g(\|\vec{x}\|) \vec{x} \Rightarrow \frac{\partial(\mathbf{f} \cdot \hat{e}_i)}{\partial(\vec{x} \cdot \hat{e}_j)} = g(\|\vec{x}\|) \delta_{ij} + g'(\|\vec{x}\|) \frac{x_i x_j}{\|\vec{x}\|} \quad (33)$$

One can see that Eqn. 32 and Eqn. 33, for the isotropic activation function’s Jacobian, contains non-diagonal terms in addition to the normal diagonalised derivative — this may increase gradient flow through these scaffold neurons, hastening their neural differentiation and operationalisation.

The way in which such neurons are initialised depends on the diagonalisation picture being considered. This is, in practicality, non-trivial, and choices can range in effect by explicit or spontaneous symmetry breaking. This arises since the reparameterisations are only functionally identical on the forward pass; they interact and are non-equivalent with gradient descent algorithms during updates. This is felt to be a very insightful direction for future study — typically, reparameterisation symmetries are equivalent on both forward and backward passes, which is not true in this setup. Moreover, after the diagonalisation procedure, the two occurrences of either \mathbf{U} on the following layer or amending the bias term, similarly for \mathbf{V} on the backwards approach, can become decoupled, especially evident under neuronal growth. All these considerations are discussed in App. D.

Both the weights and biases associated with that scaffold neuron may be initialised in a variety of ways to be discussed, with implications for learning and resulting function. In either case, the new singular values should be set to zero, yet the surrounding affine maps must also change dimensionality to accommodate this new ‘neuron’. This may require a new column or row, depending on which direction the growth acts in.

Furthermore, one may consider layer-wise expansion if suitable normalisation is present. If one normalises magnitudes to a particular distribution, to avoid anomalously strong activations, then the magnitude of those activations may be scaled down substantially using an affine map $\mathbf{W}\vec{x} + \vec{b}$, where $\mathbf{W} = \lambda \mathbf{I}_{nm}$ and $\vec{b} = \vec{0}$, where \mathbf{I}_{nm} is a rectangular-generalised diagonal identity matrix. In such a case, the original magnitude-normalised activations can be scaled down by the affine layer to a very small value. In such cases, a carefully chosen isotropic activation function may have an identity Jacobian about the origin, $\mathcal{J}_{\mathbf{f}}|_{\vec{0}} = \mathbf{I}_{n \times n}$. This is locally linear, and the prior normalisation guarantees the magnitudes will not enter a highly curved region of the activation function, so the layer becomes effectively linear. With subsequent normalisation, the affine down-scaling of magnitudes can be corrected. Without either normalisation, one could parameterise the isotropy $\mathbf{f}_*(\vec{x}; \alpha) = \alpha \vec{x} + (1 - \alpha) \mathbf{f}(\vec{x})$, $\alpha \in [0, 1]$ analogous to prior approaches [20].

3.3 Overview of Implementation

In addition to growth and pruning considerations, it must be decided when to apply them. What will be discussed is a functional buffer of neurons, consisting of two primary hyperparameters: *the number of scaffold neurons*, $\Xi \in \mathbb{Z}_+$, and *singular-value threshold*, $\vartheta \in \mathbb{R}_+$. In practicality, any prior method for pruning and growth could be implemented to various effects, and the methodology should be considered open to any such choice⁶, but this singular-value thresholding is presented primarily in this approach.

The threshold value indicates at which point the singular value connections are considered significant to performance; below this value, their inclusion is considered negligible or perhaps contributes to rarely-used, non-robust adaptations (potentially even the proposed maladaptations [15]). This threshold value would typically be chosen to be a small positive number. The number of scaffold neurons indicates the buffer of neurons which is maintained below this threshold. If it is set to $\Xi = 2$, then two scaffold neurons are maintained in the network at any time, i.e. two diagonalised neurons below the singular-value threshold⁷. If more neurons are below the threshold, then neuronal pruning can occur; if fewer, neuronal growth occurs. These can be computed every epoch or less for computational tractability — this incidentally aligns with the intermittent scheduling routine of Evci et al. [19] emerging for differing computational reasons, namely the cost of SVD diagonalisation instead of explicit gradient computations.

In the following two subsections, a step by step methodology is provided on how to prune or grow neurons in dense networks. The extension to convolution growth and pruning of kernels is exactly analogous, treating the kernels channelwise dense networks.

⁶Perhaps except for scheduled growth and pruning of a predefined number of connectivities/neurons. This would just repeatedly delete and replace the smallest singular values with zero, which appears pointless. Instead, any thresholding method, which reactively changes the amount of pruning and growth is preferable.

⁷One may consider that there remains a surprising distinction between the number of scaffold neurons, $\Xi > 1$ and $\Xi = 1$. This is because the gradients induced by isotropic primitives are non-local and explicitly depend on the dimensionality of the space, so differing Ξ are not equivalent. Similar can be said for the subsequent parameters associated with each new scaffold neuron, which have differing gradient-couplings due to symmetry-breakings and so each scaffold neuron likely diverges in specialisation and differing number of scaffold neurons does have a meaningful consequence.

3.3.1 Forward Adaption

This subsection outlines the full forward adaption process such that it can be easily implemented. The forward process is when considering an affine map $\mathbb{R}^n \rightarrow \mathbb{R}^m$, then the following layer characterised by m -dimensionality can be increased or decreased. Several of these steps and reparameterisations can be contracted for computational efficiency, whether or not these contractions are implemented affects gradient flow as discussed in *App. D*.

First perform a left-partial diagonalisation of the weight parameters using singular value decomposition, $\mathbf{W}_1 = \mathbf{U}\Sigma\mathbf{V}^T$. This reparameterises from *Eqn. 34* to *35*, as previously demonstrated⁸.

$$\mathbf{W}_2 \mathbf{f}_{\text{iso},1} \left(\mathbf{W}_1 \vec{x} + \vec{b}_1; o \right) + \vec{b}_2 \quad (34)$$

$$= \mathbf{W}_2 \mathbf{U} \mathbf{f}_{\text{iso},1} \left(\Sigma_1 \mathbf{V}^T \vec{x} + \mathbf{U}^T \vec{b}_1; o \right) + \vec{b}_2 \quad (35)$$

The dimensionality of these matrices is given by: $\mathbf{U} \in \mathbb{R}^{m \times m}$, $\mathbf{V}^T \in \mathbb{R}^{n \times n}$, $\Sigma \in \mathbb{R}_{\geq 0}^{m \times n}$, $\mathbf{W}_2 \in \mathbb{R}^{p \times m}$, $\vec{b}_1 \in \mathbb{R}^m$, $\vec{b}_2 \in \mathbb{R}^p$ and $o \in \mathbb{R}_{\geq 0}$.

The next step is to threshold the singular values to determine how many are below the threshold, ϑ . These are the entries along the diagonal.

If the number of scaffold neurons falls below the desired count, $|\{\Sigma_{ii} | \Sigma_{ii} < \vartheta\}| < \Xi$ then iteratively add neurons until the condition is equalised. This is iterative growth (neurogenesis) of the network. This is described first below with Ξ increasing by one⁹.

In this case proactive contractions of the matrices can be considered, which also highlights that the two instances of \mathbf{U} can be decoupled as shown in *Eqn. 36*, where dashes indicate the new parameterisations in contrast with the prior.

$$= \mathbf{W}'_2 \mathbf{f}_{\text{iso},1} \left(\Sigma'_1 \mathbf{V}'^T \vec{x} + \vec{b}'_1; o' \right) + \vec{b}'_2 \quad (36)$$

From this equation, one implements neurogenesis through the following steps.

1. For matrix, $\Sigma \in \mathbb{R}_{\geq 0}^{m \times n}$, a row of zeros should be appended to the bottom of the matrix to form a matrix $\Sigma' \in \mathbb{R}_{\geq 0}^{(m+1) \times n}$. This is given by $\Sigma' = \begin{pmatrix} \Sigma \\ \vec{0}^T \end{pmatrix}$
2. For vector, $\vec{b}_1 \in \mathbb{R}^m$ this is modified with a new last entry, b_* to form $\vec{b}'_1 \in \mathbb{R}^{(m+1)}$. Additionally, b_* must be chosen such that $b_*^2 + o' = o$, forming the non-negativity restriction $b_*^2 < o$. The new vector is of form $\vec{b}'_1 = \begin{pmatrix} \vec{b}_1 \\ b_* \end{pmatrix}$.
3. For scalar, $o \in \mathbb{R}_{\geq 0}$, an adjustment follows accordingly from the prior step: $o' = o - b_*^2$.
4. For matrix, $\mathbf{V}^T \in \mathbb{R}^{n \times n}$, no change need be made.
5. For matrix, $\mathbf{W}_2 \in \mathbb{R}^{p \times m}$, this matrix requires a new column $\mathbf{W}'_2 \in \mathbb{R}^{p \times (m+1)}$. The exact initialisation of this column, \vec{U}_* , does not matter for the forward pass since it does not materially alter the functionality due to the premultiplication by a zeroed singular value and if $b_* = 0$. However, in terms of a gradient coupling, this has subtle yet significant implications. Setting the column to the zero-vector can result in a spontaneous symmetry breaking upon the next optimisation step, whilst specifying a non-zero vector acts as an explicit symmetry breaking which will bias learning accordingly. There is a range of such choices, such as choosing to form a semi-orthogonal matrix by using a Gram-Schmidt procedure to produce a column that ensures semi-orthogonality of the matrix. Alternatively, initialising to be equal to an existing column or linear combination of columns may be desirable to increase fidelity around existing high singular values. A convention may be selected, such as unit-normalised vector forming a semi-orthogonal matrix, a range of equally valid degenerate options is possible, and these may couple with training dynamics unexpectedly. This will take the form $\mathbf{W}'_2 = (\mathbf{W}_2 \quad \vec{U}_*)$. This is highly interesting, as although these parameter symmetries all retain functionality in forward pass as expected, they can diverge in terms of resultant gradients, which may be unexpected, coupling differently to optimisers and resulting in later functionality divergences — a first-order broken symmetry which is preserved only upto zeroth-order, while adaptive methods break them to second-order.

⁸One does not need to undo the diagonalisation after this procedure, the basis change leaves the network functionally equivalent. Both training and diagonalising other surrounding layers will destroy the diagonalisation of the specified layer; there is no purpose in doing this manually. Although the basis change will couple differently to dynamic optimisers and certain initialisations for grown layers will prevent reversing diagonalisation exactly.

⁹Again, this threshold can be redefined to be the magnitude with respect to loss as an alternative loss-based approach, effectively a mean importance statistic over a batch. A logarithm before thresholding could be taken to make order-of-magnitude scales comparable. Overall, this is less ideal as it doesn't indicate the consequence on loss if the entire neuron is grown or pruned, only the local gradient.

6. For vector, $\vec{b}_2 \in \mathbb{R}^p$, an adjustment arising from the prior bias term can be considered: $\vec{b}'_2 + \mathbb{E}(g(\cdot)) \vec{U}_* b_* = \vec{b}_2$; therefore, $\vec{b}'_2 = \vec{b}_2 - \mathbb{E}(g(\cdot)) \vec{U}_* b_*$. Since the norm remains constant when the network grows, no additional discrepancy arises due to the non-linear norm scaling in this reparameterisation within the batch. However, choices can then be made for \vec{U}_* and b_* to ensure this is identically zero, by initialising either to the zeros. This means a spontaneous symmetry must occur in either or both variables, if set to zero; and one may be explicitly symmetry broken by being non-zero on initialisation. Approximately correct solutions can also be made for \vec{b}'_2 with respect to the batch, the discrepancy arises from $\mathbb{E}(g(\cdot))$ yet can be minimised with an appropriate normalisation such that an expected scaling is known. Then both may be explicitly symmetry broken. However, conventionally, \vec{U}_* , can satisfy the semi-orthogonality and $b_* = 0$.

Moving onto neural pruning when the number of scaffold neurons exceeds the desired count, $|\{\Sigma_{ii} | \Sigma_{ii} < \vartheta\}| > \Xi$, then iteratively prune neurons until the condition is equalised. This is iterative pruning of the network. This is described first below with Ξ decreasing by one.

1. For matrix, $\Sigma \in \mathbb{R}_{\geq 0}^{m \times n}$, the row closest approximating the zero vector, such as the smallest singular value row, may be deleted to form a matrix $\Sigma' \in \mathbb{R}_{\geq 0}^{(m-1) \times n}$. This is given by $\Sigma = \begin{pmatrix} \Sigma' \\ \vec{\Sigma}^T \approx \vec{0}^T \end{pmatrix}$
2. For vector, $\vec{b}_1 \in \mathbb{R}^m$ this is modified by deleting the last entry, b_* to form $\vec{b}'_1 \in \mathbb{R}^{(m-1)}$, $\vec{b}_1 = \begin{pmatrix} \vec{b}'_1 \\ b_* \end{pmatrix}$.
3. For scalar, $o \in \mathbb{R}_{\geq 0}$, an adjustment follows accordingly from the prior step: $o' = o + b_*^2$.
4. For matrix, $\mathbf{V}^T \in \mathbb{R}^{n \times n}$, no change need be made.
5. For matrix, $\mathbf{W}_2 \in \mathbb{R}^{p \times m}$, this matrix requires deletion of the corresponding column $\mathbf{W}_2 \in \mathbb{R}^{p \times (m-1)}$. One could similarly implement Eqn. 30 if the full-rank invertibility is satisfied. Generally this forms a new matrix, \mathbf{W}'_2 , from $\mathbf{W}_2 = (\mathbf{W}'_2 \quad \vec{U}_*)$.
6. For vector, $\vec{b}_2 \in \mathbb{R}^p$, an adjustment arising from the prior bias term can be considered: $\vec{b}'_2 = \vec{b}_2 + \mathbb{E}(g(\cdot)) \vec{U}_* b_*$, which preserves approximate functionality, accurate up to the current batch determining the non-linear g term.

4 Experimental Results

This section demonstrates preliminary performance on a range of multilayer perceptron architectures. These models offer a straightforward application of the approach demonstrated for a minimalistic setup.

They are trained using a learning rate of $\eta = 0.08$ using ADAM optimisers, batch size $n = 24$ on CIFAR10 classification, using an MLP of structure $[3072, m, 10]$ where m is specified per plot, and an elementwise input standardisation, $\mu = 0$ and $\sigma = 1$, across the CIFAR10 dataset. The activation function used is isotropic-tanh, stated in Eqn. 37, or standard tanh, stated in Eqn. 38 (written multivariately), for cases explicitly stated as anisotropic.

$$\mathbf{f}(\vec{x}) = \tanh(\|\vec{x}\|) \hat{x} \quad (37)$$

$$\mathbf{f}(\vec{x}; \hat{e}_i) = \sum_i \tanh(\vec{x} \cdot \hat{e}_i) \hat{e}_i \quad (38)$$

The dynamic adaptations are applied to pretrained multilayer perceptron networks, then training is advanced whilst using a dynamic adaptation scheduler, changing by ± 1 neuron per epoch, then when reaching the desired width, training is continued until reaching a 48 epochs of additional training, where accuracy stagnation is empirically observed.

The first plot, Fig. 3, takes trained networks using isotropic-tanh and then adapts their widths dynamically during post-training. There are 16 repeats per network, over 16 network permutations, corresponding to a total of 256 unique multilayer-perceptron networks. For each of the four starting widths, there are 16 repeats, and these are the same network instances as starting points in the dynamical network post-training across each starting width for consistency.

One can observe that all networks smoothly transition between widths as expected by the dynamical network implementation, which identically preserves function for neurogenesis and closely approximates it for neurodegeneration. Only for a degenerating width to 8 neurons does accuracy typically decline, otherwise performance remains relatively unchanged.

Consistent performance when varying between 16, 24 and 32 neurons is insightful, as it is suggestive that the networks learn very similar functions which are detrimentally little by small amounts of neurodegeneration. Furthermore, the 32 width layer begins at a higher accuracy, and maintains this for 16 and 24 width networks, suggesting an initial overabundance of neurons, followed by neurodegeneration, is beneficial for performance. This incidentally aligns strongly with biological neural network findings [9], which suggests an advantage of an initial overabundance of neurons.

Similar to Fig. 3, Fig. 4 shows the same networks but organised such that each plot shows the final widths grouped.

Overall, from Fig. 4, one can observe that neurodegeneration to 8 neurons results in an accuracy drop across all networks, whilst neurogenesis from 8 neurons to 16, 24 or 32 results in a gradual increase in accuracy — suggesting the network was bottlenecked.

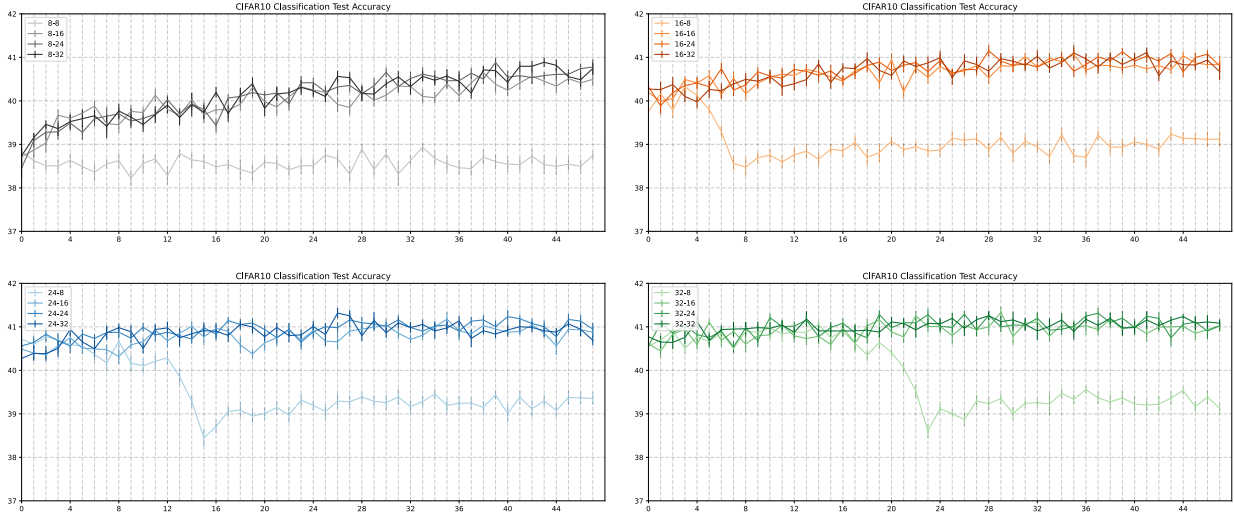


Figure 3: All plots demonstrate accuracy on CIFAR10 classification of pretrained multilayer perceptron networks, which go through an additional 48 epochs of training as their architecture is dynamically adapted. Top-left shows networks with an initial width of 8 hidden layer neurons, going through neurogenesis to 8, 16, 24 or 32 width layers. Similarly, the top-left plot demonstrates results beginning at 16 neurons, the bottom-left at 24 neurons and the bottom-right at 32. The larger networks undergo neurogenesis, no change, or neurodegeneration depending on whether the width increases, remains the same or decreases, respectively.

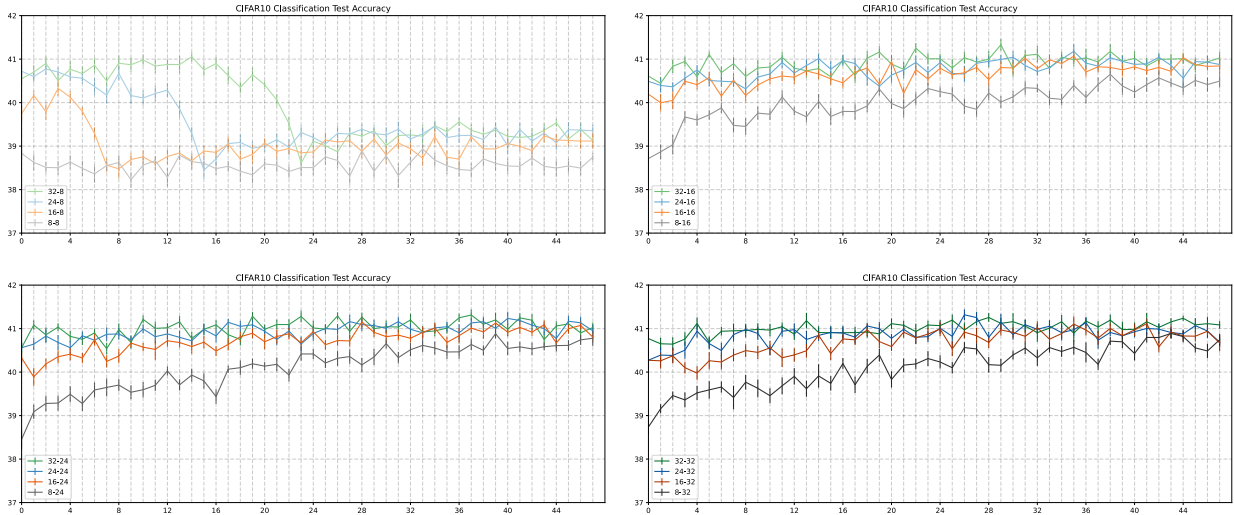


Figure 4: All plots demonstrate accuracy on CIFAR10 classification of pretrained multilayer perceptron networks, which go through an additional 48 epochs of training as their architecture is dynamically adapted. The top-left shows networks with a final width of 8 hidden layer neurons, going through neurodegeneration from 8, 16, 24 or 32 width layers. Similarly, the top-left plot demonstrates results finishing with 16 neurons, the bottom-left at 24 neurons and the bottom-right at 32.

Finally, *Fig. 5*, display these networks alongside their initial pretraining accuracies. In addition, it also displays identical networks using anisotropic tanh as an ablation comparison.

In all cases, isotropic tanh displays significantly higher accuracy than its anisotropic, standard tanh counterpart, demonstrating that on CIFAR10 classification, the newly formulated isotropic primitives are not detrimental but beneficial. This echoes earlier preliminary results for reconstruction tasks [17]. This persists even given the decline in performance for 8 neuron final widths, which themselves have a reduction in performance.

5 Conclusion

Overall, this work introduces a practical procedure for dynamical networks given isotropic primitives defined through orthogonal equivariance. Results are provided which show that neurodegeneration and neurogenesis do not cause catastrophic forgetting under architecture adaptations, by preserving identically (neurogenesis) or well-approximating

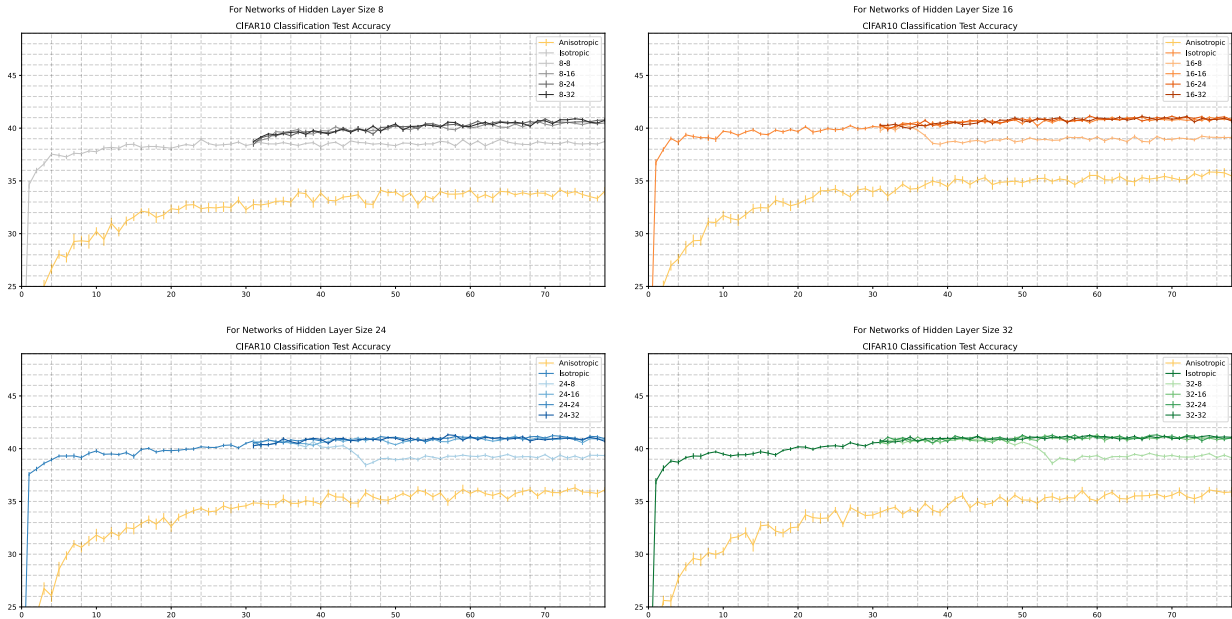


Figure 5: Displays, identical plots to Fig. 3 in the same layout, but also displays the 24 epoch pretraining and the anisotropic tanh control network.

(neurodegeneration) existing function. Furthermore, additional properties such as exact function invariances under asymptotic 50% sparsity is demonstrated theoretically.

The primary conceptual contribution is an ontological inversion between the nature of neurons and their associated symmetries, which is then leveraged to allow such dynamical behaviour in continuous-group equivariant defined primitives.

Future work can explore the merger of networks with differing functions through isotropic dynamical networks, as well as knowledge sharing between tasks in continual learning settings. Encouraged is an exploration into other symmetry-prescribed approaches to determine model biases stemming from such redefinitions, and leveraging the behaviour of these for improved modelling.

References

- [1] Caleb J. Axelrod, Swanne P. Gordon, and Bruce A. Carlson. Integrating neuroplasticity and evolution. *Current Biology*, 33(8):R288–R293, Apr 2023. ISSN 0960-9822. doi: 10.1016/j.cub.2023.03.002. URL <https://doi.org/10.1016/j.cub.2023.03.002>.
- [2] Wei Wen and Gina G Turrigiano. Keeping your brain in balance: homeostatic regulation of network function. *Annual review of neuroscience*, 47, 2024.
- [3] Pico Caroni, Flavio Donato, and Dominique Muller. Structural plasticity upon learning: regulation and functions. *Nature Reviews Neuroscience*, 13(7):478–490, 2012.
- [4] Jyoti Mishra and Adam Gazzaley. Cross-species approaches to cognitive neuroplasticity research. *NeuroImage*, 131: 4–12, 2016. doi: 10.1016/j.neuroimage.2015.10.013. URL <https://doi.org/10.1016/j.neuroimage.2015.10.013>.
- [5] Chiara La Rosa and Luca Bonfanti. Brain plasticity in mammals: An example for the role of comparative medicine in the neurosciences. *Frontiers in Veterinary Science*, 5:274, 2018. doi: 10.3389/fvets.2018.00274. URL <https://doi.org/10.3389/fvets.2018.00274>.
- [6] Ioanna Dori, Chrysanthi Bekiari, Ioannis Grivas, Anastasia Tsingotjidou, and Georgios C Papadopoulos. Birth and death of neurons in the developing and mature mammalian brain. *The International Journal of Developmental Biology*, 66(1-2-3):9–22, 2021.
- [7] Anthony Holtmaat and Karel Svoboda. Experience-dependent structural synaptic plasticity in the mammalian brain. *Nature Reviews Neuroscience*, 10(9):647–658, 2009.
- [8] Martin M Riccomagno and Alex L Kolodkin. Sculpting neural circuits by axon and dendrite pruning. *Annual review of cell and developmental biology*, 31(1):779–805, 2015.
- [9] Carolin Scholl, Michael E Rule, and Matthias H Hennig. The information theory of developmental pruning: Optimizing global network architectures using local synaptic rules. *PLoS computational biology*, 17(10):e1009458, 2021.
- [10] Gina G Turrigiano and Sacha B Nelson. Hebb and homeostasis in neuronal plasticity. *Current opinion in neurobiology*, 10(3):358–364, 2000.
- [11] Dmitri B Chklovskii, BW Mel, and K Svoboda. Cortical rewiring and information storage. *Nature*, 431(7010): 782–788, 2004.
- [12] Warren S McCulloch and Walter Pitts. A logical calculus of the ideas immanent in nervous activity. *The bulletin of mathematical biophysics*, 5(4):115–133, 1943.
- [13] Héctor J. Sussmann. Uniqueness of the weights for minimal feedforward nets with a given input-output map. *Neural Networks*, 5(4):589–593, 1992. ISSN 0893-6080. doi: [https://doi.org/10.1016/S0893-6080\(05\)80037-1](https://doi.org/10.1016/S0893-6080(05)80037-1). URL <https://www.sciencedirect.com/science/article/pii/S0893608005800371>.
- [14] Vijay Badrinarayanan, Bamdev Mishra, and Roberto Cipolla. Understanding symmetries in deep networks, 2015. URL <https://arxiv.org/abs/1511.01029>.
- [15] George Bird. Isotropic deep learning: You should consider your (foundational) biases, May 2025. URL <https://doi.org/10.5281/zenodo.15476947>.
- [16] George Bird. The spotlight resonance method: Resolving the alignment of embedded activations. In *Second Workshop on Representational Alignment at ICLR 2025*, 2025. URL <https://openreview.net/forum?id=alxPpqVRzX>.
- [17] George Bird. Emergence of quantised representations isolated to anisotropic functions, 2025. URL <https://arxiv.org/abs/2507.12070>.
- [18] George Bird. From directed graphs to deep learning - a symmetry-first approach, August 2025. URL <https://doi.org/10.5281/zenodo.16912528>.
- [19] Utku Evcı, Trevor Gale, Jacob Menick, Pablo Samuel Castro, and Erich Elsen. Rigging the lottery: Making all tickets winners, 2021. URL <https://arxiv.org/abs/1911.11134>.
- [20] Tao Wei, Changhu Wang, Yong Rui, and Chang Wen Chen. Network morphism. In *International conference on machine learning*, pages 564–572. PMLR, 2016.

- [21] George Cybenko. Approximation by superpositions of a sigmoidal function. *Mathematics of control, signals and systems*, 2(4):303–314, 1989.
- [22] Kurt Hornik, Maxwell Stinchcombe, and Halbert White. Multilayer feedforward networks are universal approximators. *Neural networks*, 2(5):359–366, 1989.
- [23] Kurt Hornik. Approximation capabilities of multilayer feedforward networks. *Neural Networks*, 4(2):251–257, 1991. ISSN 0893-6080. doi: [https://doi.org/10.1016/0893-6080\(91\)90009-T](https://doi.org/10.1016/0893-6080(91)90009-T). URL <https://www.sciencedirect.com/science/article/pii/089360809190009T>.
- [24] Nelson Elhage, Tristan Hume, Catherine Olsson, Nicholas Schiefer, Tom Henighan, Shauna Kravec, Zac Hatfield-Dodds, Robert Lasenby, Dawn Drain, Carol Chen, et al. Toy models of superposition. *arXiv preprint arXiv:2209.10652*, 2022.
- [25] Tianqi Chen, Ian Goodfellow, and Jonathon Shlens. Net2net: Accelerating learning via knowledge transfer, 2016. URL <https://arxiv.org/abs/1511.05641>.
- [26] Utku Evci, Yani A. Ioannou, Cem Keskin, and Yann Dauphin. Gradient flow in sparse neural networks and how lottery tickets win, 2022. URL <https://arxiv.org/abs/2010.03533>.
- [27] Xavier Glorot and Yoshua Bengio. Understanding the difficulty of training deep feedforward neural networks. In *Proceedings of the thirteenth international conference on artificial intelligence and statistics*, pages 249–256. JMLR Workshop and Conference Proceedings, 2010.
- [28] Kaiming He, Xiangyu Zhang, Shaoqing Ren, and Jian Sun. Delving deep into rectifiers: Surpassing human-level performance on imagenet classification, 2015. URL <https://arxiv.org/abs/1502.01852>.
- [29] Alston S Householder. A theory of steady-state activity in nerve-fiber networks: I. definitions and preliminary lemmas. *The bulletin of mathematical biophysics*, 3(2):63–69, 1941.

A Conceptual Background: Generalising Functional Forms Through Prescriptive Symmetries

The functional forms used throughout the dynamic architecture methodology are non-standard, e.g. not elementwise but continuous symmetry-derived, and this section provides justification for this generalisation. Continuous-symmetry-defined functional forms are necessary for this approach to dynamic topologies. This section motivates it generally; however, the theoretical sections assume only specifically the orthogonal-derived ‘isotropic forms’ [15, 17] in derivations.

This section begins by discussing why elementwise functional forms were originally introduced as an analogue of biological systems, then how they can be generalised through a symmetry-led approach, and, finally, an overview of how this broadens the resulting computational class. This is largely discussion-based; a mathematics-based description is provided in the theoretical background section of *Sec. 2*.

A.1 Implicit Constraints on Contemporary Functional Forms

Qualitatively, one may define the computational system termed ‘neural networks’ as a computation predicated upon individual units intercommunicating, through numerical values mapped through functions, to yield an overall desirable, learnt function. This situates the role of neurons in these models, with their interconnections and computations, as the primary constraint on the functional forms of the neural network computation system. This perspective is especially evident historically [12] where it is explicitly stated, whereas it has now become more of an understated constraint.

In artificial settings, this yields the machine learning regime generally termed “artificial neural networks” or “deep learning” when extended in depth. Hence, this machine learning approach is characterised by these delineated artificial neurons, as the chosen functional form classes reflect this presupposed neural unit — typically applying functions to (decomposed) elements termed ‘neurons’. Collectively, these individual neurons communicate, and maps adapt to reproduce the desired function through collective computation [12, 21, 22, 23]. Overall, those primitive maps, underpinning the neural computation approach, circularly reinforce the impression of the individuated neuron from which they were conceptually derived. Particularly when considered multivariately, the chosen functions often individuate neurons by distinguished directions [24, 15, 17], introducing a basis-dependence.

Such assumptions in functional forms extend to most primitives in widespread use, including, but not limited to, the majority of: activation functions, normalisers, optimisers, several regularisers, operations, approaches in gradient clippings and more [15] — these collectively reinforce this neuron-wise approach and exhibit a (neuron-)basis-dependence. The pervasiveness of contemporary primitives may be due to a number of factors: historical naturalistic ideals about neural computation systems, appealing to their biological counterparts for intuition and inspiration, whilst overlooking the neural unit as a physical limitation due to cellular individuality. From this inspired foundation, the form may then be reinforced by subsequent software and hardware alignment, positive performance precedent, and perhaps also cognitive entrenchment [15]. Overall, the approach is implicitly constrained by the composition of individuated neurons with their associated functional-form computations. These typically serve as the atomic units for forming ever-larger networks within the functional class of artificial neural networks.

Yet mathematically, the individuality of neurons is assumed into implicit constraints on the possible functional forms — a form chosen conceptually, not by mathematical necessity. Hence, the current form of network primitives, introducing neuron individuality, serves solely as a conceptual limitation on this form of computation system, not a fundamental one, and is therefore open to generalisation.

Overall, the question arises: must elementwise functional forms be central to design, if not by mathematical necessity? More generally, if implicit basis dependence is introduced without clear justification, since it is often obfuscated and thus inadvertent, are symmetry-led generalised functional forms equal in justification to implement?

Universal approximation theorems do not resolve the first consideration [21, 22, 23], since they were developed as a posteriori theoretical support justifying such forms after this choice had already become normative. Hence, they do not provide proof of a unique ability exhibited by the elementwise functional form.

This positions the isotropic primitives as an alternative formulation that can be reasonably explored, and they represent one instance of a continuous-symmetry generalisation of functional forms. Moreover, only through a continuous-defined set of primitives, distinct from elementwise practice, is this form of dynamic topology enabled, as it is predicated on continuous basis changes enabling diagonalisation.

This broader perspective is discussed, as it is crucial that all instances introducing such basis-dependence be redefined to deindividuate the neuron in this approach to dynamic topologies and motivates the reformulation undertaken. However, by departing from these implicit constraints, allows considerations that naturally broaden the overall functional class of neural models and offer a wider conceptual contribution than dynamic topologies alone. This could be considered to generalise the overall computational system of “artificial neural networks” beyond biological and cellular constraints — and offers a generalised and underexplored design axis in neural models design for follow-up evaluation.

A.2 Functional forms relation to Reparameterisation Invariance

Derived from current formulations, one can work *deductively* to determine the computational equivalences [13, 14] that are inherent to most networks. Exhibited by such models are parameter-space degeneracies, usually centred around the exchange of neurons — formally termed a permutation symmetry, S_n , of the neurons in the network. Under appropriate

reparameterisations, permuting neurons by exchanging corresponding internal weights and biases can be considered a computational invariance of the network¹⁰.

Intuitively, the network functions identically before and after the exchange induced by permuting actions. Hence, a permutation symmetry is *deduced* from this current construction. This deduction is a consequence of contemporary functional forms, which themselves conceptually arose from the constraint of an individuated neuron as the units comprising neural models.

A.3 Inverting the Explanatory Direction: Symmetries lead to Neurons

This work argues that such a perspective on individuated neurons and their resultant constraints on functional forms is limiting, and alternatives are underarticulated and thus underexplored.

This work achieves generalisation by replacing the conceptual neuron-based computation with a symmetry-principled foundation from which conventional functional forms can be recovered, as well as more general reformulations. This uses symmetries not as descriptive categorisations associated with existing phenomena, but rather *prescriptively* to enable new, desired functional forms with associated behaviours, such as differing parameter invariances, and representational biases [16, 17]. From such considerations, unique properties of these generalised neural models emerge, including the dynamic network possibility highlighted in this work.

Instead of considering how permutation-like symmetries are deduced alongside other associated permutation-like groups, such as hyperoctahedral $B_n = \mathbb{Z}_2^n \times S_n$ and others, from current functional forms constrained conceptually by individuated neurons, it is proposed to invert this relation, thereby enabling prescriptive symmetry use. Alongside the enabled generalisation, it is argued that this constitutes a preferable foundation for functional forms, where admitted formulations are derived rather than conceptually motivated.

This work reverses the process: instead of working deductively from *neurons leading to symmetry*, this work proposes reconsidering the observed relation in reverse: *symmetry leads to neurons*. The exact formulation is provided in *Sec. 4* and motivates the isotropic form. Below highlights how such a relation can be used in reverse as a prescribed-symmetry foundation:

Currently: Notion of Neurons in a Network \rightarrow Primitive Functional Forms \rightarrow Deduced Symmetries
Proposed: Prescribed Symmetries \rightarrow Novel Primitive Functional Forms \rightarrow Generalised Notions of
 ‘Neurons’ \rightarrow Enriched Functional Class of Neural Models

This situates primitive symmetries as foundational for the functional form and hence ontologically prior. Neurons emerge as a notion derived from these foundations through functional forms. Hence, neurons emerge as a concept from the mathematical structure induced by the symmetry prescription, namely through distinguished directions induced by the representation of the symmetry. This demonstrates how symmetry prescriptions become fundamental rather than the conceptual notion of neurons in a network.

For example, in this reversed framing, current networks emerge from a single, implicitly chosen symmetry: the permutation group S_n , producing an associated primitive functional form that decomposes the activation vector in the standard basis, which provides the conventional notion of individual neurons. Yet embracing the reversal allows other symmetries to take the place of permutations, generating new forms for primitives and, hence, the induced notion of neurons. This demonstrates the generalisation enabled and the broadening of the existing computational class of artificial neural networks, as prescribed symmetries can be substituted to yield different functional forms, which can then be composed into a broader repertoire of models.

A.4 Leveraging Novel Behaviours of Networks defined by Continuous Symmetries

In this picture, the notion of individuated neurons becomes an emergent property of the implicit permutation *definitions* in current primitives. Using this reversed ontology, one can instead consider neurons as a unit extending from the permutation definition, rather than the other way around. From this, a natural next step is to substitute alternative symmetries, yielding new sets of primitives and, consequently, new notions of what a neuron is.

This work focuses on leveraging one such alternative symmetry-defined branch to demonstrate possibilities. Primarily explored is the ‘isotropic’ redefinition [15, 17], predicated on the continuous orthogonal symmetry $O(n)$, instead of the canonical discrete permutation subgroup $S_n \subset O(n)$. From this, primitive sets emerge that are equivariant to standard representations of these orthogonal actions.

Utilised: Orthogonal Symmetry \rightarrow Isotropic Functional Forms \rightarrow Deindividuated Neurons
 ‘Deindividuated’ = ‘Basis-independent’ Generalised Neurons \rightarrow Diagonalise Bases \rightarrow Dynamic Architectures

Using this inversion, one can now work deductively to rediscover emergent neurons, where isotropic networks have a more general notion of a neuron. Typically, we may consider a layer construction as n copies of 1-dimensional neuron-like objects concatenated, *due to permutation symmetry*; however, under the orthogonal symmetry redefinition, this shifts to considering a layer as 1 copy of an n -dimensional neuron. The fundamental qualitative ‘neuron’ is higher-dimensional and

¹⁰This is also connected to the symmetries of the *discrete* directed graphs underlying the communication pathways between models predicated on discrete, individuated neurons.

can be continuously decomposed into any linear combination, provided it is normalised, to yield equally valid alternative individuated bases. Yet this framework means that the resulting mathematics no longer depends on any particular basis.

Crucially, in this basis-independent approach, there is no longer a clear, individuated and agreeable definition of a neuron. There effectively exists a (global) gauge freedom to choose any decomposition of individual neurons one likes; there is no mathematical boundary that delineates each unit. This shifts the modular object from a neuron to a layer. Any choice of individual neurons is no more fundamental than any other; they may continuously shift arbitrarily in definition due to their continuous orthogonal nature.

Hence, varied decompositions do not alter the computation when interspersed between affine maps, yielding familiar computational invariances under affine composition. Moreover, this freedom to change the basis of the representation space extends to circumstances in which one can project into a higher-dimensional space without loss of functionality (a neurogenesis ability). Similarly, under more restricted conditions¹¹, one can down-project to subspaces with minimal functional consequences or catastrophic failure, providing the network with neurodegenerative/pruning ability — all of which are enabled through this symmetry-principled approach.

Hence, this is a novel leveraging of computational invariance enabled by continuous symmetry redefinitions — one in which the architectural structure becomes plastic and adaptable to tasks through reparameterisations, not just the exchangeable and scalable numerical values of existing parameters. Hence, automorphisms for networks emerge that preserve function identically under architectural changes.

This contrasts with the contemporary permutation definition, which is limited to exchange symmetries which do not alter the underlying architecture. Primitive symmetries, neural architecture and functional invariance can become beneficially intertwined. Hence, this new definition of primitives enables networks to expand and contract dynamically in response to demand. This is considered a beneficial consequence directly enabled by the orthogonal reformulation of the network’s basic constituents.

This paper explores such reparameterisations, allowing neurons within a layer to compensate for alterations to the structure while maintaining functionality. One can also generalise this beyond isotropic functions to any continuous group-defined primitive sets, unlike the traditional discrete-defined permutation primitives. Orthogonal (isotropic) definitions are just used to operationalise this concept.

Although briefly featured, the approach to be discussed does not primarily reside within the approach of sparsifying a preexisting architecture [19]. Rather, it can best be described through altering both neuron number and connectivity, which are analytically ensured to reproduce the function under certain reparameterisations. Hence, it aligns thematically with other works [25, 20] where the central objective is to truly alter network topology whilst preserving functionality, rather than masking effectively preexisting graph connections.

However, except for the unifying objective, it is distinct both mathematically and in implementation from prior approaches, such as diverging through diagonalisation and a thresholded singular-value-based approach. Hence, it contrasts with a static-nodal underlying directed graph method, allowing a dynamic nodal graph. A more thorough comparative analysis between prior works is given in *App. B*

B Extended Related Work

In this section, a comparison to other approaches for dynamic network architecture will be undertaken, with a summary of each followed by key similarities and differences.

Rigged-Lottery (RigL) This paper [19] approaches dynamic topologies by training a sparse network which periodically and efficiently prunes or grows based on a set of criteria. This paper applies such techniques to weight parameters, likely because those parameters tensors grow bilinearly with network size, whilst not for linearly growing parameter tensors such as biases or batch-normalisation coefficients — these are explicitly argued to be computationally negligible. This is because the central principle of this work is to produce a computationally efficient sparse network from a predefined larger architecture, where unpruned weights may otherwise constitute the largest overhead.

In summary, the dynamic topology aspect of RigL consists of two primary two steps, the dropping and growing of connections. Methodologically, this primarily consists of a zero-masking to an predefined, underlying directed graph, where preexisting connectivities are enabled/disabled in the resulting sparse network. The dropped connections are those which have the minimum magnitude within the network; hence, in the forward pass one could argue that they contribute the least significant change to the loss¹². For growth, the full dense gradients are calculated for that layer, particularly those for which the sparsity mask is currently zeroed, i.e. absence of a connection. From these, the connections which would produce the largest gradient correction are unmasked within the sparse network, at an initialised value of zero to ensure existing network functionality is retained in the forward pass, since it effectively matches its preexisting value due to sparsity masking which to all intents and purposes made it an untrainable zero-valued parameter. This gradient approach, centers around these unmasked connections having the largest contribution to reducing the loss in the subsequent timestep. Follow-on work [26] establishes the consequences and implications of gradient-flow on this sparsity approach to varying topologies, with a heterogenous connectivity generalisation of Glorot/He initialisation [27, 28].

¹¹One that weight-decay regularisations may further moderate.

¹²Although strictly, this is not guaranteed as compensatory large weights could reamplify such a signal in subsequent layers. Such an approach would need explicit computation of a before-and-after loss for every parameter adaptation, which has a large compute burden.

Overall, this is a successful approach, but diverges substantially in both aims and implementation to this paper. The primary focuses contrasts between a finding an efficient sparse network within a predefined network architecture using a sparsity mask on an underlying directed graph, compared to what I argue is a full dynamic topology where the underlying graph may also change in both edge connectivity and nodes. In this work, sparsity is not the primary concern¹³. Implementationally, they also diverge: where RigL prunes the bottom- k weights based upon magnitude, with an explicit k -parameter (which can dynamically change), this paper’s method uses symmetry reparameterisations and thresholded singular values to determine which neurons are to be pruned. An explicit growth/prune number within this paper, would not make sense due to the breakdown of neuron individuality, and a shift between discrete connectivities and more continuous maps with variable dimensionality. Despite this, some implementation details such as the drop-grow intermittent update are also employed in this work, although instead emerging from an effort to mitigate the increased computational cost of diagonalisation. In summary, the work proposed is better situated within the neurode/genesis approach to dynamic topologies, rather than masking connectivity for sparsity — although, the latter may be still just as applicable, if not better (due to the interpretable and orthogonal decompositions), to isotropic networks and could also be explored.

Net2Net this pair of techniques [25], “Net2WiderNet” and “Net2DeeperNet”, approaches the problem of neurogenesis by initialising a larger-only architecture, either wider or deeper. It is initialised such that it preserves the functionality of the smaller network. Therefore, one effectively transfers the knowledge from one smaller system to another larger system from initialisation, or informally embeds the smaller network within the larger one.

For the Net2WiderNet algorithm, this largely consists of appending new columns to one layer’s weight matrix which are cloned from columns of the original matrix. A corresponding row is added to the subsequent weight matrix of the following layer. This results in a column-wise and subsequent row-wise multiplicity for the layers, which is counteracted by a rowwise division by that multiplicity, the “replication factor” in the subsequent layer. Such actions produce a wider network that is functionally equivalent.

Geometrically, this amounts to embedding the prior activations within a larger vector space, with the multiplicity resulting in a diagonal-like embedding. To the same effect, one could also use multiplicative factors $\sum_i \alpha_i = 1$ for the new rows to continue leaving the function identical, corresponding to differing embeddings. Moreover, due to the replication, the column-wise addition is degenerate in both forward and backward pass; therefore, differentiating gradients do not cause such columns to diverge in parameterisation — it remains function preserving without additional noise. Hence, this necessitates some gradient-based noise to be introduced to the system to cause symmetry-breaking to the otherwise degenerate columns. This noise is discussed in terms of dropout, or noise on the new column’s parameterisations, among other possibilities. Crucially, the latter produces only an approximate function preserving neurogenesis. However, this could have been similarly mitigated by a non-degenerate column and zeroed subsequent weight — this is employed in the present work, ensuring full functional invariance without necessity for symmetry breaking degrading functional equivalence. This was also highlighted in follow-on work [20].

Net2DeeperNet adds a layer using an identity matrix and a strong constraint to idempotent-restricted activation functions $\phi \circ \phi = \phi$, this is already satisfied by Rectified Linear Units [29], but not so for most other activation functions. Follow on work continued to explore the expanding morphisms [20] which preserve network functionality, such as learnable parameterised activation functions which can become linear in depth-wise addition, $\psi(\vec{x}; \alpha) = \alpha\vec{x} + (1 - \alpha)\psi(\vec{x})$. The network morphing equations for enlarged width also converge on an analogous constraint, in the pointwise non-linear case, to the ones proposed in this paper. In short, additional columns can be added with a corresponding multiplicative factor of zero to counteract any functional change, preserving the invariance pointwise; however, this is not as trivial for the case of isotropy where activation functions cause interdependence between activations requiring the preceding additional column to be zeroed. Hence, the relations presented in this paper can be thought to reproduce network morphing equations but for isotropic functions. In generality, the network morphology considerations could be considered retrospectively as an extension to existing parameter symmetry work, stemming from the preexisting permutation primitives and reparameterisations, similarly to how the present work stems from isotropic primitives and its reparameterisations with affine compositions.

Generally similarities arise thematically through the shared central goal: to have neurogenesis within an architecture without loss of functionality to the network. Hence, column-wise addition does draw some parallels with the technique to be presented; however, remaining within the current individuated neuron paradigm and without reconceptualising primitives and neurons through symmetry to leverage specific reparameterisations. In some regards the approach differs between a more discrete addition of neurons towards a more continuous approach, exploiting spectral decomposition of networks to add and remove neurons with fewer functional implications.

Their method consists of a neurogenesis-like effect, where new columns are appended, but crucially neurodegeneration is not included. Additionally the Net2Net approach is limited to anisotropy and does not use the diagonalisable approach, since anisotropic networks do not feature this symmetry. Any rowwise initialisations of the subsequent layer can also be undertaken within this paper without forward-pass consequence, and additionally intrinsic length parameter enables a broader flexibility to reparameterisations for changing topologies. neurodegeneration, enabled through one-to-one connectivity pruning, is also a core feature of the this paper. This is uniquely aided by the available diagonalisation

¹³However, reparameterisations of every layer may be jointly optimised to increase sparsity whilst preserving function if desirable, in such an arrangement additional connectivity pruning can be undertaken with some change to function.

procedure enabled by rejecting the premise of individuated neurons. Overall, this means that the two methods approach dynamic topologies with a natural, shared goal of function preservation, and some analogous constraints for up-projection, but diverge substantially in theoretical considerations and mathematical implementations, with additional actions enabled by the isotropic approach which is reliant on a symmetry-principled approach to the problem.

C Recursive View of Generalised Isotropy: Nested Functional Classes and Hyper-Spherical Shell Collapse

The purpose of this section was initially to demonstrate the effect of normalisation on this structure. The intention is to reduce degradation in performance, through normalisations by reducing errors when $\Sigma_{ii} = \epsilon$ for some small, but non-zero epsilon.

However, it is instead determined that a isotropic generalised-dense network displays a nested functional class due to its inherent symmetry.

In this construction, one can consider an isotropic neural network as the following series, with $\mathbf{f}_{\text{iso}}(\vec{x}) = g(\|\vec{x}\|)\vec{x}$

$$\vec{x}^{(2)} = \mathbf{W}_2 \mathbf{f}_{\text{iso}} \left(\underbrace{\left(\mathbf{W}_1 \vec{x}^{(0)} + \vec{b}_1 \right)}_{\vec{x}^{(1)}} \right) + \vec{b}_2 \quad (39)$$

$$\vec{x}^{(2)} = \mathbf{W}_2 g \left(\left\| \mathbf{W}_1 \vec{x}^{(0)} + \vec{b}_1 \right\| \right) \left(\mathbf{W}_1 \vec{x}^{(0)} + \vec{b}_1 \right) + \vec{b}_2 \quad (40)$$

$$\vec{x}^{(2)} = g \left(\left\| \vec{x}^{(1)} \right\| \right) \mathbf{W}_2 \mathbf{W}_1 \vec{x}^{(0)} + g \left(\left\| \vec{x}^{(1)} \right\| \right) \mathbf{W}_2 \vec{b}_1 + \vec{b}_2 \quad (41)$$

$$\vec{x}^{(2)} = g \left(\left\| \vec{x}^{(1)} \right\| \right) \mathbf{W}'_2 \vec{x}^{(0)} + g \left(\left\| \vec{x}^{(1)} \right\| \right) \vec{b}'_1 + \vec{b}_2 \quad (42)$$

Similarly with increasing layers:

$$\vec{x}^{(3)} = \mathbf{W}_3 g \left(\left\| \vec{x}^{(2)} \right\| \right) \vec{x}^{(2)} + \vec{b}_3 \quad (43)$$

$$\vec{x}^{(3)} = \mathbf{W}_3 g \left(\left\| \vec{x}^{(2)} \right\| \right) \left(g \left(\left\| \vec{x}^{(1)} \right\| \right) \mathbf{W}'_2 \vec{x}^{(0)} + g \left(\left\| \vec{x}^{(1)} \right\| \right) \vec{b}'_1 + \vec{b}_2 \right) + \vec{b}_3 \quad (44)$$

$$\vec{x}^{(3)} = g \left(\left\| \vec{x}^{(2)} \right\| \right) g \left(\left\| \vec{x}^{(1)} \right\| \right) \mathbf{W}'_3 \vec{x}^{(0)} + g \left(\left\| \vec{x}^{(2)} \right\| \right) g \left(\left\| \vec{x}^{(1)} \right\| \right) \vec{b}'_1 + g \left(\left\| \vec{x}^{(2)} \right\| \right) \vec{b}'_2 + \vec{b}_3 \quad (45)$$

Generalising this to yield the full isotropic dense network recursive relation.

$$\vec{x}^{(l)} = \left(\prod_{i=1}^{l-1} g \left(\left\| \vec{x}^{(i)} \right\| \right) \right) \mathbf{W}_l^\circ \vec{x}^{(0)} + \sum_{i=1}^{l-1} \vec{b}_i^\circ \prod_{j=1}^i g \left(\left\| \vec{x}^{(j)} \right\| \right) + \vec{b}^\circ \quad (46)$$

The angular dependence may appear trivial due to the $\mathbf{W}_l^\circ \vec{x}^{(0)}$; however, this is misleading due to it also appearing in the argument of map, g , the output angular distribution non-trivially depends on the input. However, interspacing other maps besides isotropic and affine primitives may also be explored from this view.

Moreover, this can be rewritten under suitable parameter changes as *Eqn. 47*. Relaxing the reparameterisation constraint for *Eqn. 47* and enabling parameters to take any values also broadens the notion of a dense neural network in this context, showing that isotropy generalised networks can act as a perturbative sum of decreasing sized networks. Therefore, this generalised construction enables a nested functional class and hence expressivity inclusion, much like the nested functional classes of Residual networks yet instead emerging from symmetry. Furthermore, the intermediate layers can vary in dimensionality whilst still preserving this nested functional class structure, this symmetry emergence of nested functional classes stems from primitive constraints not architectural constraints; therefore it does not constrain the layer dimensionality like Residual Networks classically do.

$$\vec{x}^{(l)} = \sum_{i=1}^{l-1} \left(\mathbf{W}_i^\circ \vec{x}^{(0)} + \vec{b}_i^\circ \right) \left(\prod_{j=1}^i g \left(\left\| \vec{x}^{(j)} \right\| \right) \right) \quad (47)$$

To make clear, this is not a classical dense network but is a larger encompassing but derivative architecture including it as an enclosed functional class — hence, it generalises classical dense networks. It displays a natural nested functional class, and a perturbative-like expansion which can recursively includes shallower networks. If $g : \mathbb{R}_+ \rightarrow [0, \alpha]$, then this also acts like a perturbative expansion, allowing convergence if $\alpha \leq 1$. Similarly normalisation can be used to implement a series convergence. This approach may also allow a new route to recursive reimplementations of backward and forward propagation methods. It is applicable for any non-linearity which can be expressed as $\mathbf{f}(\vec{x}) = g(\vec{x})\vec{x}$ for $g : \mathbb{R}^n \rightarrow \mathbb{R}$ or similarly for complex networks. This includes any generalised norm-based term, such as hyperoctahedral primitives

defined using an l -norm for $l \neq 2$, although isotropy's orthogonal equivariance ensures this. Generalising further, one could substitute independent networks for each g argument producing an ensemble network-like effect.

The initial intention was to show the application of normalisation to this system and how this may mitigate the input-error under pruning if placed carefully.

One may consider how the residual input error term from pruning neurons, after residual bias has been gauged away, may continue to negatively impact performance. One could consider pre- or post-composing activation functions with a hyper-spherical normalisation such that each layer produces a vector with a fixed norm.

This can be seen to be an undesirable placement, despite mitigating the input-error under pruning, since all the non-linearities become constant and the layer becomes linear and equivariant under reparameterisation to Eqn. 48 — which is guaranteed not to have a universal approximation theorem due to the constraint to affine maps. This suggests this form of hyperspherical shell normalisation collapses expressibility to affine maps.

$$\vec{x}^{(l)} = \mathbf{W}\hat{x}^{(0)} + \vec{b} \quad (48)$$

Therefore, normalising to a hyperspherical shell must *not* happen occur within an isotropic layer, as this guarantees linear expressibility by the network.

Instead, either generalised normalisation, which does not project to the hyperspherical shell such as the proposed Chi-Normalisation [15], which can be pre- or post-composed with isotropic activations which is likely a preferable form of normalisation. These constrain the magnitude of \vec{x}_i in the product $\Sigma_{ii}\vec{x}_i$, to ensure that as $\Sigma_{ii} \rightarrow 0$ it cannot be compensated by a growth in \vec{x}_i which may otherwise adversely affect the network's functionality.

Generally, one should also consider the pre- or post- composure of normalisations that can also impact vanishing or exploding gradients within these generalised isotropic architectures.

D Reparameterisation Non-Equivilance Through Gradient Coupling

Although function equivilance is retained through the various reparameterisations, these reparameterisations are non-equivilant when considering gradient updates.

The most trivial case, which appears to occur uniquely in isotropic-enabled orthogonal reparameterisations is coupling to adaptive optimisers. In effect, although a diagonalised network performs equally to its non-diagonalised counterpart, since adaptive optimisers often use an elementwise scaling, then the result trajectories are not equivariant to the orthogonal actions — these networks will learning substantially differently. Thus, they diverge in function equivilance through training. This phenomena should not be underappreciated, since this gradient trajectory divergence does not typically happen in anisotropic reparameterisations.

Ordinarily this would not be relevant under parameter symmetries; however, the isotropic parameter symmetries do cause these adaptive optimiser (elementwise) accumulations to diverge, meaning that isotropic parameter symmetries are only valid to first order in this case. This is a new consideration for the nature of parameter symmetries in networks with generalised primitives.

The second trivial case of gradient coupling is products, $\mathbf{A}\mathbf{B} = \mathbf{W}$. If diagonalisation methods do not recontract terms, then gradient trajectories will also diverge. Considering $\vec{y}_m = \mathbf{W}_{mn}\vec{x}_n$ and $\mathbf{A}\mathbf{B} = \mathbf{W}$, produces two differing update equations, assuming standard gradient descent, as shown in Eqns. 49 and 50. Other optimisers yield analogous results and the author is unaware of an optimiser, or an existence possibility, which natively reconciles these. Notating $g_p = \frac{\partial \mathcal{L}}{\partial y_p}$

$$\vec{y}'_m = \mathbf{W}'_{mn}\vec{x}_n = (\mathbf{W}_{mn} - \eta g_m \vec{x}_n) \vec{x}_n \quad (49)$$

$$\vec{y}'_m = (\mathbf{A}'_{mk}\mathbf{B}'_{kn}) \vec{x}_n = (\mathbf{A}_{mk} - \eta g_m \mathbf{B}_{ki}\vec{x}_i) (\mathbf{B}_{kn} - \eta g_j \mathbf{A}_{jk}\vec{x}_n) \vec{x}_n \quad (50)$$

Subtracting these equations to determine the divergence with $\epsilon_m = (\mathbf{W}'_{mn} - \mathbf{A}'_{mk}\mathbf{B}'_{kn}) \vec{x}_n$. These are displayed in Eqns. 51 and 52.

$$\epsilon_m = (\mathbf{W}_{mn} - \eta g_m \vec{x}_n) \vec{x}_n - (\mathbf{A}_{mk}\mathbf{B}_{kn} - \eta g_m \mathbf{B}_{ki}\vec{x}_i - \eta g_j \mathbf{A}_{jk}\mathbf{A}_{mk}\vec{x}_n + \eta^2 g_j g_m \mathbf{A}_{jk}\mathbf{B}_{ki}\vec{x}_n\vec{x}_i) \vec{x}_n \quad (51)$$

$$\epsilon_m = \eta (g_m \mathbf{B}_{kn}\vec{x}_n \mathbf{B}_{ki}\vec{x}_i + g_j \mathbf{A}_{jk}\mathbf{A}_{mk}\vec{x}_n\vec{x}_n - g_m \vec{x}_n\vec{x}_n (1 + \eta g_j \mathbf{A}_{jk}\mathbf{B}_{ki}\vec{x}_i)) \quad (52)$$

This result establishes that leaving a layer in a partially diagonalised parameterisation may cause divergences if $\Sigma \mathbf{V}^T$ are not contracted back to \mathbf{W} . Moreover, various reparameterisations $\mathbf{W} = \mathbf{A}\mathbf{B} = \mathbf{C}\mathbf{D}$ may cause differing trajectories, which remains pertinent to the linear aspects of isotropic functions, including in the expansion given in App. C.

However, what is more significant is the null-like reparameterisations appearing under $\Sigma_{ii} = 0$ as previously discussed. These leave the network functionally identical; yet reparameterisations can be couple to the optimisation in non-trivial ways. This may allow a new mode to steer such networks, acting like a new choice situated somewhere between a reparameterisation and initialisation. This can be discusd both as a foward and backward process, but the forward partial diagonalisation is displayed in Eqn. 53 for consideration.

$$\vec{y}_i = \mathbf{W}_{ij} \left[\mathbf{f}_{\text{iso},1} \left(\underbrace{\sum_{jk} \mathbf{V}_{lk} \vec{x}_l}_{\mathbf{Y}_{jl}} + \vec{b}_j \right) \right]_j + \vec{d}_i \quad (53)$$

Differentiating \vec{y} with respect to \mathbf{Y} , \mathbf{W} and \vec{b} , indicates their interdependency, and how initialisation even for rows/columns corresponding to zero-singular values has a non-trivial gradient coupling, producing a symmetry breaking consideration. These are given in *Eqns.* 54, 55 and 56, respectively using notation $\vec{z}_j = \sum_{jk} \mathbf{V}_{lk} \vec{x}_l + \vec{b}_j$.

$$\frac{\partial \vec{y}_i}{\partial \mathbf{Y}_{mn}} = g(\|\vec{z}\|) (\mathbf{W}_{im} \vec{x}_n) + \mathbf{W}_{ij} \vec{z}_j \frac{\partial}{\partial \mathbf{Y}_{mn}} g(\|\vec{z}\|) \quad (54)$$

$$\frac{\partial \vec{y}_i}{\partial \mathbf{W}_{mn}} = \delta_{mi} g(\|\vec{z}\|) (\mathbf{Y}_{nl} \vec{x}_l + \vec{b}_n) \quad (55)$$

$$\frac{\partial \vec{y}_i}{\partial \vec{b}_m} = g(\|\vec{z}\|) \mathbf{W}_{im} + \mathbf{W}_{ij} \vec{z}_j \frac{\partial}{\partial \vec{b}_m} g(\|\vec{z}\|) \quad (56)$$

One can see that in all these equations, the choices of reparameterisation for entries premultiplied by $\Sigma_{ii} = 0$ still have a meaningful coupling to optimisation and therefore gradient trajectories. Therefore, these null-like reparameterisations only preserve forward pass network functionality, whilst altering the backward pass gradient step. Therefore, these parameter symmetries are preserved upto zeroth order but not first order. One can observe that *Eqn.* 55 will become relevant after two gradient steps when the update makes the original zero singular value become non-zero.

This has ramifications for the initialisation choices under neurogenesis. Various choices for initialisations can result in spontaneous symmetry breaking if zero initialised, or one can bias gradient trajectories using a non-zero initialisation which performs an explicit symmetry break into the backward pass. These considerations may be important aspects of dynamical networks moving forward and the potential for parameter symmetries to only maintain the symmetry upto zeroth order should be studied and findings factored into such implementations. These may steer learning without immediately altering the network. These appear to generally manifest when a reparameterisation is available which preserves network functionality, but that action is outside the group actions defining the primitives. Overall this is a function invariance under parameter symmetries, whilst gradient coupling breaks the optimisation symmetry and hence the networks are inequivalent under these reparameterisations.